NASA/TM–2021–0017040

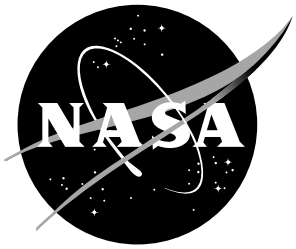

Temperature and Frequency Dependent Electrical Properties of AVCOAT and Shuttle Tile Material

Mark A. Nurge
NASA, Applied Physics Laboratory, Kennedy Space Center, Florida

Robert C. Youngquist
NASA, Applied Physics Laboratory, Kennedy Space Center, Florida

June 2021

NASA STI Program. . . in Profile

Since its founding, NASA has been dedicated to the advancement of aeronautics and space science. The NASA scientific and technical information (STI) program plays a key part in helping NASA maintain this important role.

The NASA STI Program operates under the auspices of the Agency Chief Information Officer. It collects, organizes, provides for archiving, and disseminates NASA's STI. The NASA STI Program provides access to the NASA Aeronautics and Space Database and its public interface, the NASA Technical Report Server, thus providing one of the largest collection of aeronautical and space science STI in the world. Results are published in both non-NASA channels and by NASA in the NASA STI Report Series, which includes the following report types:

- TECHNICAL PUBLICATION. Reports of completed research or a major significant phase of research that present the results of NASA programs and include extensive data or theoretical analysis. Includes compilations of significant scientific and technical data and information deemed to be of continuing reference value. NASA counterpart of peer-reviewed formal professional papers, but having less stringent limitations on manuscript length and extent of graphic presentations.
- TECHNICAL MEMORANDUM. Scientific and technical findings that are preliminary or of specialized interest, e.g., quick release reports, working papers, and bibliographies that contain minimal annotation. Does not contain extensive analysis.
- CONTRACTOR REPORT. Scientific and technical findings by NASA-sponsored contractors and grantees.
- CONFERENCE PUBLICATION. Collected papers from scientific and technical conferences, symposia, seminars, or other meetings sponsored or co-sponsored by NASA.
- SPECIAL PUBLICATION. Scientific, technical, or historical information from NASA programs, projects, and missions, often concerned with subjects having substantial public interest.
- TECHNICAL TRANSLATION. English-language translations of foreign scientific and technical material pertinent to NASA's mission.

Specialized services also include organizing and publishing research results, distributing specialized research announcements and feeds, providing information desk and personal search support, and enabling data exchange services.

For more information about the NASA STI Program, see the following:

- Access the NASA STI program home page at `http://www.sti.nasa.gov`
- E-mail your question to `help@sti.nasa.gov`
- Phone the NASA STI Information Desk at 757-864-9658
- Write to:
  NASA STI Information Desk
  Mail Stop 148
  NASA Langley Research Center
  Hampton, VA 23681-2199

NASA/TM–2021–0017040

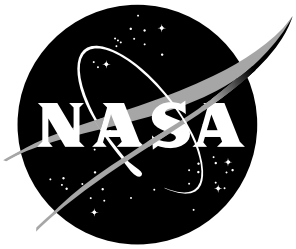

Temperature and Frequency Dependent Electrical Properties of AVCOAT and Shuttle Tile Material

Mark A. Nurge
NASA, Applied Physics Laboratory, Kennedy Space Center, Florida

Robert C. Youngquist
NASA, Applied Physics Laboratory, Kennedy Space Center, Florida

National Aeronautics and
Space Administration

John F. Kennedy Space Center
Kennedy Space Center, Florida, 32899

June 2021

Available from:

NASA STI Program / Mail Stop 148
NASA Langley Research Center
Hampton, VA 23681-2199
Fax: 757-864-6500

Abstract

This technical memorandum presents the temperature and frequency dependent electrical properties of virgin AVCOAT, charred AVCOAT, and various Shuttle Thermal Protection System (TPS) tile coatings. This data was collected to support a NASA Engineering and Safety Center (NESC) assessment team investigating the source of thermocouple anomalies in both Shuttle TPS material and AVCOAT used for on the Orion spacecraft for Exploration Flight Test 1 (EFT-1).

Contents

List of Figures

1 Summary

This technical memorandum presents the data and results from a series of tests performed on AVCOAT, charred AVCOAT, and different Shuttle Thermal Protection System (TPS) tile coatings to determine their electrical properties as a function of temperature and frequency. Initially, the samples were assumed to be insulators and the complex permittivities were measured from data collected by sandwiching each sample between two conductors to form a sandwich. However, the AVCOAT sample data showed that the material becomes conductive as it begins to char. To get an accurate conductivity reading on these charred samples, a four-point resistance probe was used to collect data. Overall, this testing showed that the virgin AVCOAT starts out as a material that is a good insulator but transitions to one with a conductivity on the order of 1860 S/m as it chars. The deeper layers of AVCOAT (un-charred) all exhibited a temperature and frequency dependence that is possibly indicative of a dielectric relaxation in the material. As the sample temperatures were increased, a knee appears in the real permittivity data sets below 1 kHz. Both the real permittivity and resistivity drop up to several orders of magnitude yet show that the material remains an insulator.

The Shuttle High Temperature Reusable Surface Insulation (HRSI) tile coatings studied included Reaction Cured Glass (RCG), Aluminum Enhanced Thermal Barrier (AETB), and Toughened Unipiece Fibrous Insulation (TUFI). The purely glass fiber parts of the tile were removed leaving only the outer layers containing just the coating. The data collected shows that the RCG, AETB, and outermost layer of the TUFI have similar electrical properties. The real permittivity plots show that there appears to be a relaxation that shows up at frequencies below 1 kHz. The relaxation frequency increases with increasing temperature. Also, the real permittivity increases up to about a factor of four between room temperature and 650K. Likewise, the resistivity (related to the imaginary permittivity) decreases up to five orders of magnitude over the same temperature interval, but still remains an insulator.

This data was collected to support a NASA Engineering and Safety Center (NESC) assessment team investigating the source of thermocouple anomalies in both Shuttle TPS material and AVCOAT used for on the Orion spacecraft for Exploration Flight Test 1 (EFT-1). The details of their findings will be documented in a separate report with this document serving as a reference.

2 Background

A Novocontrol Concept 40 Broadband Dielectric Spectroscopy system was used to make the majority of the measurements described in this document. It is capable of measuring the complex permittivity of materials from 1 μHz-3 GHz, and a temperature range of 113-673K. The system measures the complex capacitance after sandwiching the sample between a pair of electrodes. Since the geometry is known, the geometric dependence is easily removed to get to the complex permittivity. The complex permittivity is made up of a real part, ϵ' and an imaginary part, ϵ". By convention, they combine as $\hat{\epsilon} = \epsilon' - i\epsilon''$. The real portion is equal to the permittiv-

ity of free space times the relative permittivity, ϵ'=$\epsilon_0\epsilon_r$ and the imaginary portion is proportional to the conductivity, ϵ"= σ/ω, where σ is the frequency dependent conductivity and ω is the angular frequency. Both the real and imaginary parts may exhibit variations due to changes in frequency or temperature. In the plots shown in this report, the real permittivity has the permittivity of free space removed and is actually ϵ_r. The imaginary part is primarily shown as resistivity, ρ, where $\rho = 1/\sigma$.

This method works well for materials that are primarily insulators when values of ϵ" are small. However, as the imaginary part gets much larger than the real part as in the case of a conductor, the contact resistances between the capacitor measurement electrodes and the sample can become a significant source of error. So, in cases where the sample became conductive (e.g., charred AVCOAT) the resistance measured with the Novocontrol spectrometer may be dominated by contact resistances and should be treated as an upper bound, not as a fixed accurate value. There are a few methods of reducing the contact resistance - using a conductive silver paint to coat the sample or using conductive silver impregnated rubber sheets between the sample and electrodes. However, these both have drawbacks and can introduce errors, especially as the temperature increases. Consequently, a Lucas Labs Pro 4 four point probe was used to measure the resistivity more accurately. The compromise with the Lucas Labs Pro is that it is only suitable for making room temperature measurements as it isn't designed to operate in an environmental chamber at extreme temperatures.

3 AVCOAT Temperature and Frequency Dependent Electrical Properties

AVCOAT samples were measured with a Novocontrol Concept 40 Broadband Dielectric Spectroscopy system at Kennedy Space Center in early 2014 as part of a study looking into development of new dielectric non-destructive evaluation techniques for spaceflight materials. The AVCOAT samples were provided by Erik Takacs of Textron Systems in the form of a witness block that was used to train technicians. The AVCOAT is injected into a honeycomb that is an insulator composed of E-Glass with an epoxy/phenolic resin. A photo of the block and one of the samples appears below in Figure 1. It is believed that this material is similar to that which was used in the Orion EFT-1.

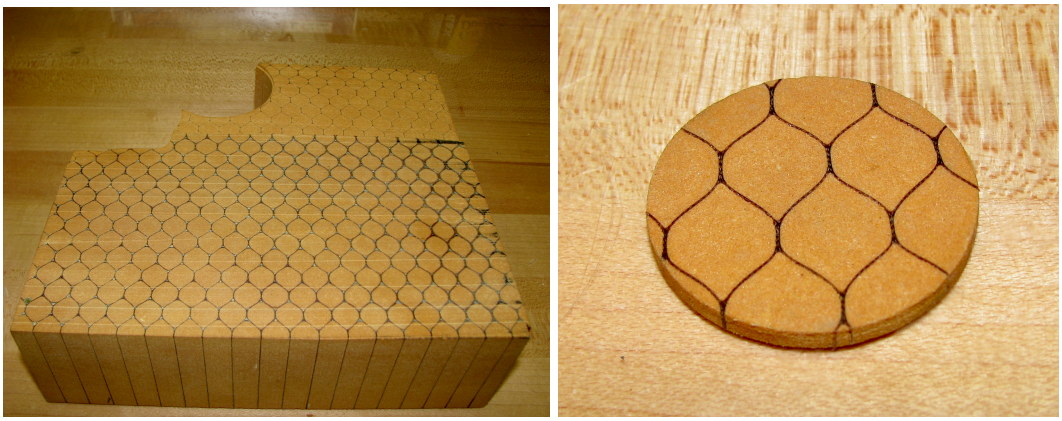

Figure 1. Block of AVCOAT used to crate samples on left. Sample used for testing shown on right.

The samples in this study were exposed to different forms of accelerated weathering but included a control for comparison. The overall results are documented in NASA TM-2014-218398. To support the NESC study, only the data from the control samples was used to plot the electrical properties of the AVCOAT as a function of both frequency and temperature. Figure 2 is the real portion of the permittivity with the permittivity of free space removed. Figure 3 is the specific resistance of the material which is computed from the imaginary portion of the permittivity measurement. Both plots show the data for the sample starting at room temperature then dropping to 153K and stepping up through 403K in 50K steps and then ending at room temperature. Three ambient temperature data sets are collected at different places in the temperature scan sequence to see if moisture in the sample bakes out and changes the measurements in any way. In this case, the three sets all appear to be similar. The rise in permittivity below 1 kHz for several of the curves is due to a sub-1 Hertz relaxation in the AVCOAT that begins to show up at higher frequencies as the temperature is raised. There are corresponding drops in the specific resistance (although not as pronounced) at similar frequencies due to

this phenomenon.

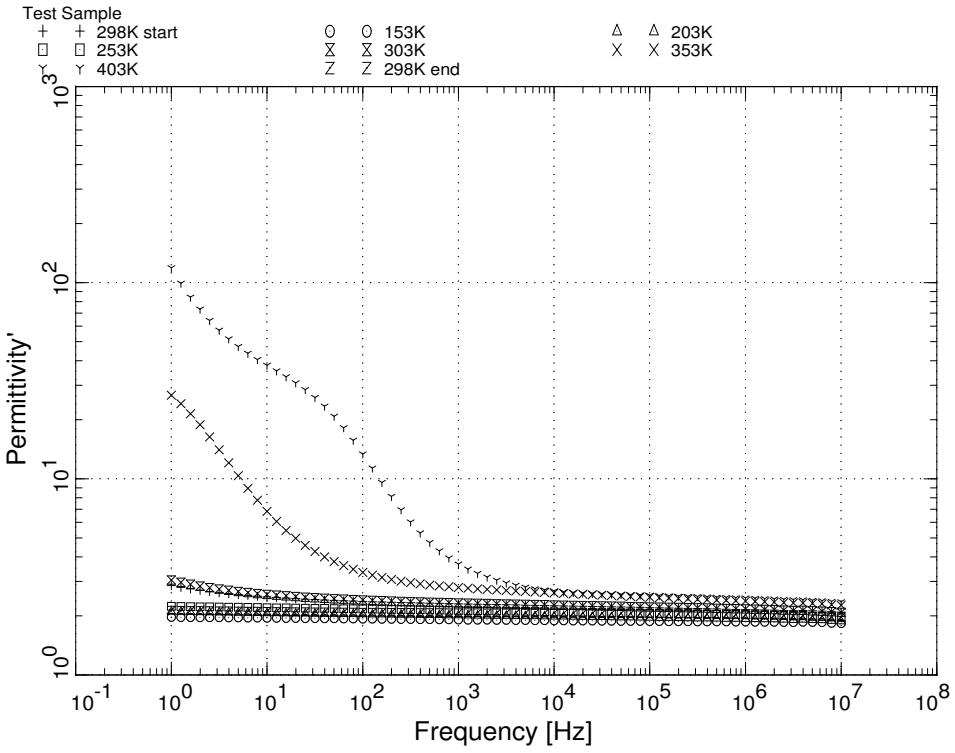

Figure 2. Plots showing the permittivity of AVCOAT as a function of frequency and temperature.

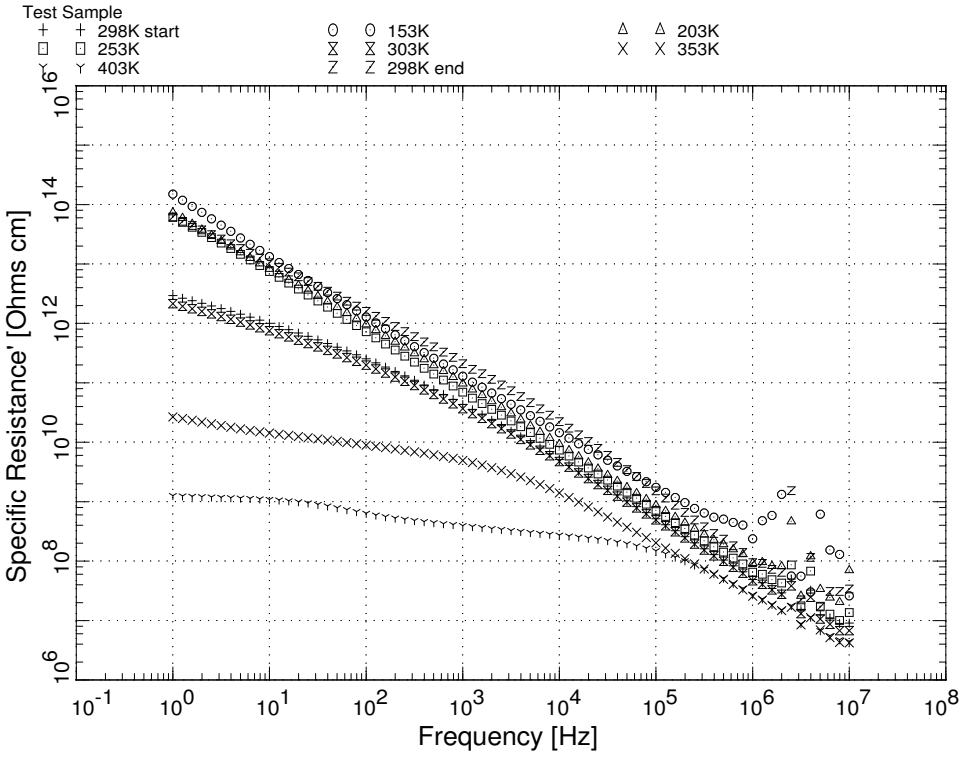

Figure 3. Plots showing the resistivity of AVCOAT as a function of frequency and temperature.

4 Charred AVCOAT Temperature and Frequency Dependent Electrical Properties

A charred AVCOAT sample from EFT-1 analog heat shield was measured with a Novocontrol Concept 40 Broadband Dielectric Spectroscopy system at Kennedy Space Center to determine electrical properties as a function depth, frequency, and temperature. The AVCOAT had been charred at an arc jet facility that ablated the outer 0.5 mm of the virgin material. Two cylindrical core samples (40 mm in diameter and around 22.6 mm thick) were removed from the larger block of charred AVCOAT that was collected from site 162 of the EFT-1 analog heat shield (ref. Figure 4 below).

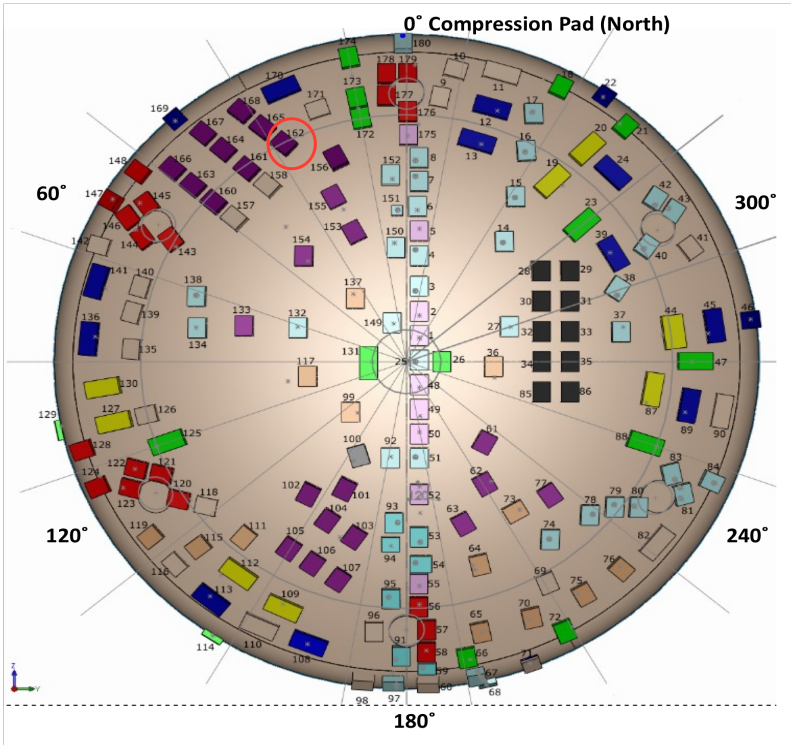

Figure 4. Diagram showing the different sample locations on the EFT-1 heat shield. Site 162 (circled in red) is the location of the charred AVCOAT sample used for these tests. This image was created by the US government and is used with permission from Jeremy Vander Kam/ARC-NASA.

The photo in Figure 5 shows the profile of a typical cylindrical core prior to cutting and a drawing showing the approximate depths of color transitions in the sample. One of the cores was then separated into 7 layers of approximately 1-2 mm thickness with around a 0.8 mm kerf in between layers leaving a remnant of about 7.8 mm. The 2nd sample was divided into 4 layers of about 1-2 mm with a 11.5 mm remnant. Some of the samples in each core broke badly during machining so that

they couldn't be used in testing. So, the samples below are taken from a mixture of the two cores. The approximate depths the sample was cut from are given in the associated figures assuming a virgin sample (adding back in the 0.5 mm ablated material).

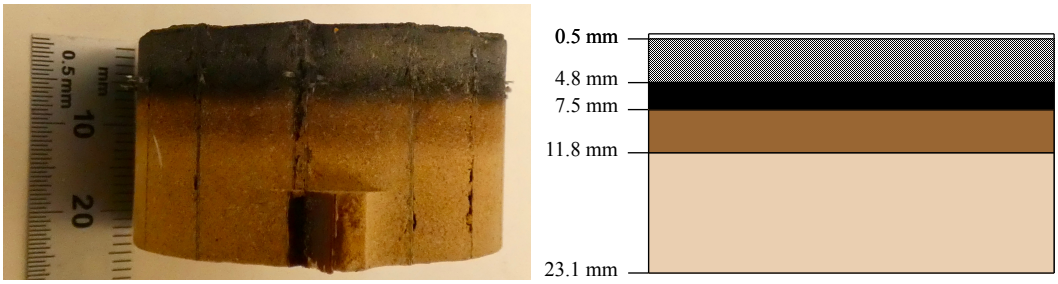

Figure 5. Photograph of a cylindrical plug cut from the charred AVCOAT showing the color changes (left). The diagram on the right shows the depth of the color changes with respect to the uncharred sample.

The complex capacitance is measured using a parallel plate capacitor with the sample sandwiched between two test electrodes. The material properties are then calculated from the data based on the known electrode geometry. The frequency range scanned was 1 Hz-10 MHz, but some of the data sets were noisy above 1 MHz and the accuracy of the data in those regions suffers. In those cases, the suspect data was deleted from the plots. Each sample was heated from 300K-650K in 50K steps. A final measurement at 300K would normally be used to see if the sample returned to its starting value. However, the AVCOAT would off-gas as the temperature reached the high end of the range and many samples remained stuck to the auxiliary measurement electrodes at the completion of the test. Since the material was altered by heating, the final 300K scans were erratic and it was decided not to include them here. The temperature profile data wasn't saved for the first five samples, but the plots for sample layers 6 and 7 shown below in Figure 6 are highly similar and can be considered to be representative of the other samples.

The upper layers of black charred AVCOAT exhibit conductive behavior and the results are no longer reliable as contact resistance between the electrodes and sample becomes dominant. For these samples, a four point conductivity probe was needed to make an accurate measurement. At the point where the samples change from being all black to black on one side and tan on the other (layer 3), the resistivity and real permittivity begin exhibiting characteristics of an insulator.

4.1 Results - Layer 1

Figure 7 shows photos of both sides of the upper layer of the charred AVCOAT. The fiberglass honeycomb matrix appears to have deteriorated faster than the epoxy novolac resin, leaving cracks and crevices which make the charred layer fragile. While this is a probably a desirable trait for an ablator, it made it difficult to cut the outer

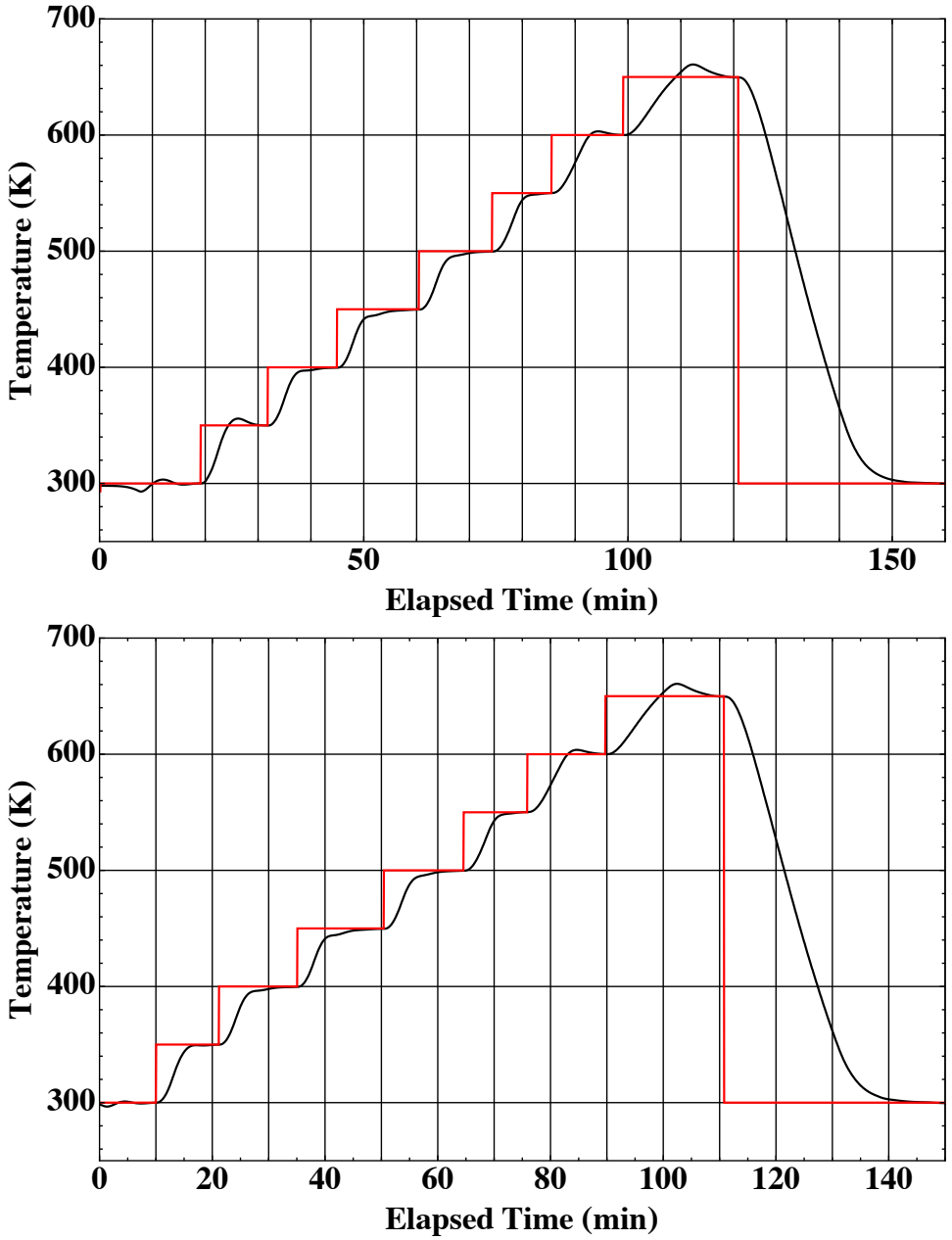

Figure 6. The upper plot shows the temperature profile of layer 6 while the lower plot shows the temperature profile for layer 7. The red curve shows the set temperature, and the black is the sample temperature. These two sets of plots are highly similar and can be considered representative of the profiles for layers 1-5.

layers of the sample without breaking into pieces.

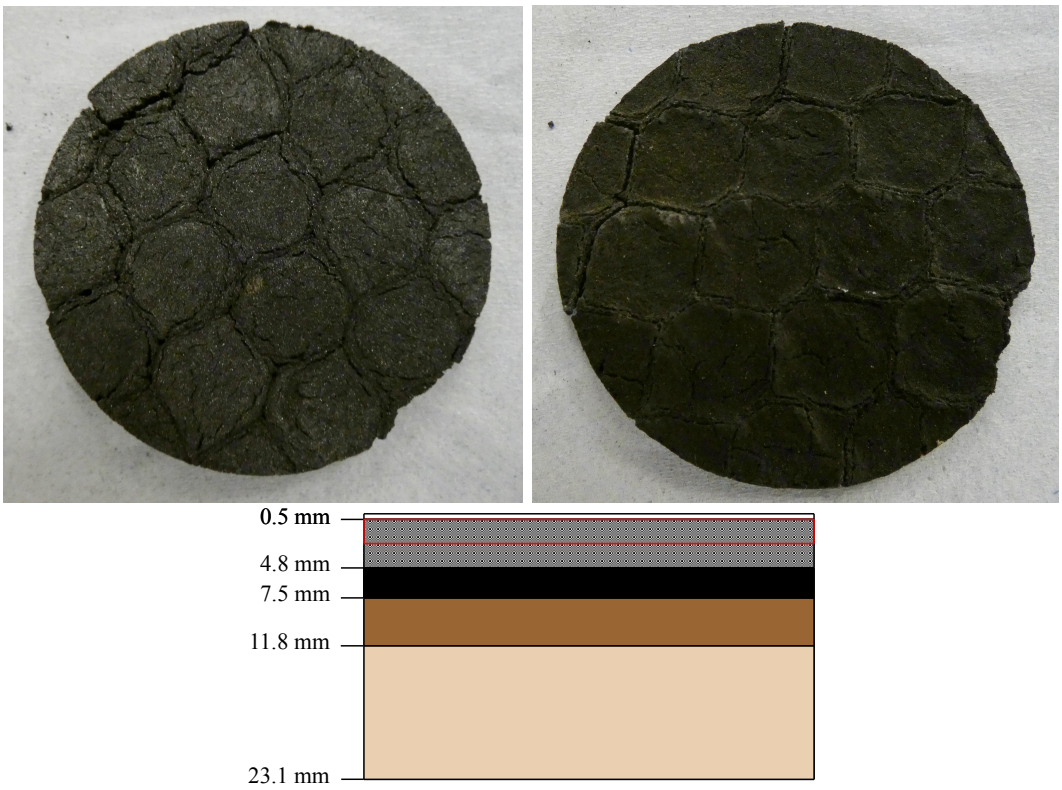

Figure 7. Photos showing both sides of a sample cut from the outermost layer of charred AVCOAT taken from a section of the analog heat shield for EFT-1. The sample is about 40 mm in diameter and 2.1 mm thick. The red box in diagram below shows the approximate location the sample was taken from within the cylindrical core (0.5 mm from the original surface).

When measuring conductive samples like these outer layers, the error bars displayed while making the measurement where excessive for the real relative permittivity giving no meaningful data. Therefore, the plot for the real relative permittivity is not presented to minimize confusion. The deviations shown in the resistivity plot in Figure 8 also had large error bars for the data measured at frequencies above around 20 kHz. It can be seen that the resistivity varied from around 4 Ω-cm to around 5.7 Ω-cm. It's possible some of this variation is due to deformation of the sample as it was heated. It off-gassed at the higher temperatures and in some cases, stuck to the electrodes.

4.2 Results - Layer 2

Figure 9 shows photos one side of the charred AVCOAT from layer 2 (just below the surface). The deterioration of the fiberglass honeycomb combined with its smaller

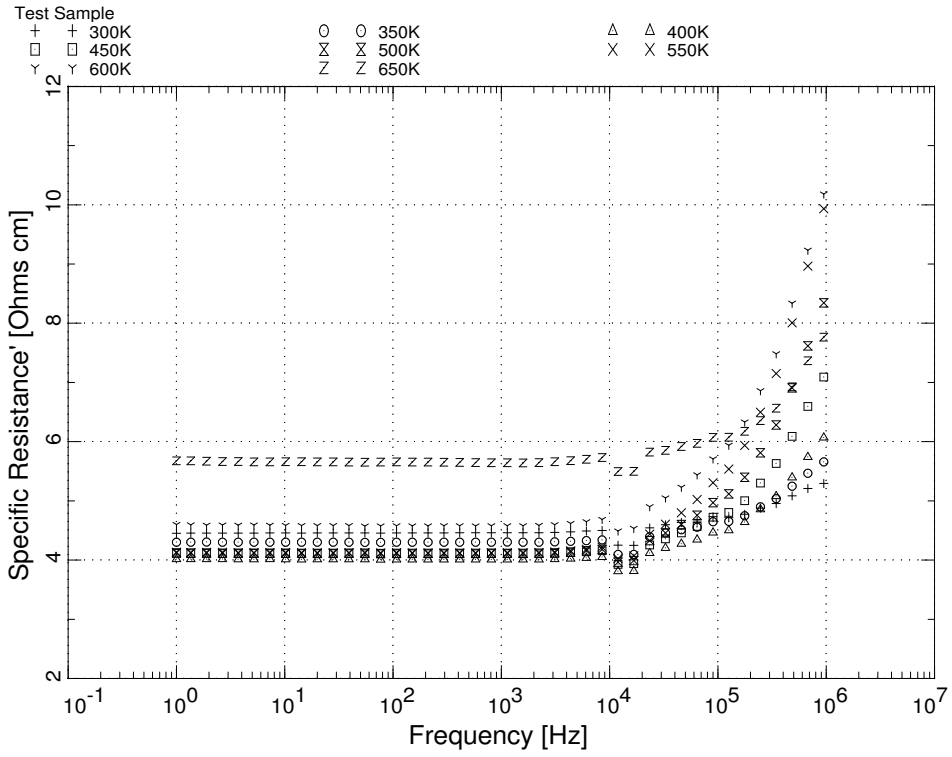

Figure 8. Resistivity of layer 1 as a function of frequency and temperature.

thickness resulted in the 40 mm sample breaking into smaller pieces. As a result, a smaller (12 mm) diameter set of test electrodes was used to measure the electrical properties.

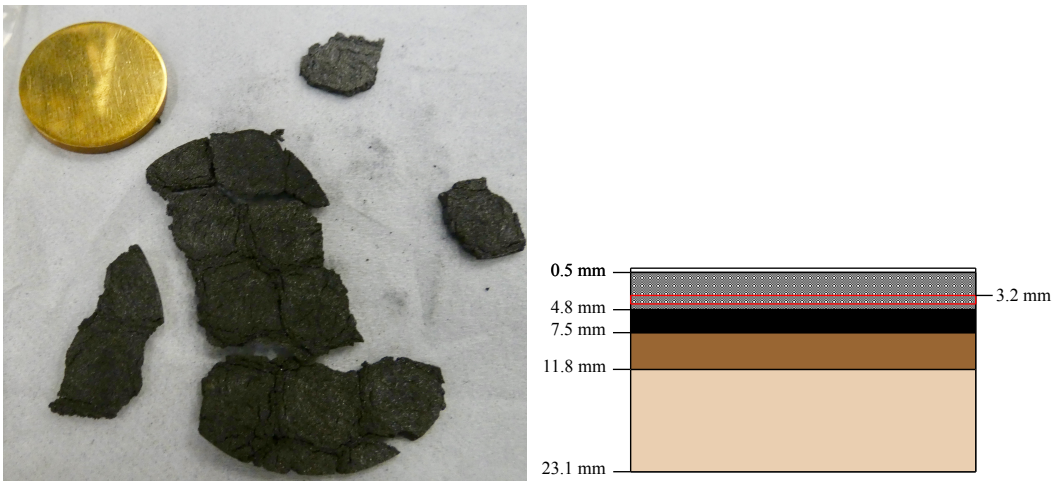

Figure 9. Photo showing one side of a sample cut from the layer 2 of charred AVCOAT taken from a section of the analog heat shield for EFT-1. The sample was about 40 mm in diameter and 1.0 mm thick but broke apart requiring the use of a smaller set of measurement electrodes (shown in photo) to make the measurements. The diagram on the right shows the approximate location the sample is from within the cylindrical core (3.2 mm from original surface).

As with layer 1, the materiel behaves as a conductor and the measurement of the real permittivity is not meaningful. The deviations shown in the resistivity plot in Figure 10 also had large error bars for the data measured at frequencies above around 20 kHz. It can be seen that the resistivity remained consistently 1-2 Ω-cm.

4.3 Four-point Probe Measurement

Since the samples of charred AVCOAT in the previous two subsections only represent an upper bound for resistivity due to contact resistances, a Lucas Labs Pro 4 four-point probe system was used to make a room temperature resistivity measurement on a larger block of charred AVCOAT. A photo of the system is shown below in Figure 11.

The system was configured manually to provide a constant 100 mA current to the outer probe tips and the voltage was read off the inner probe tips with the Keithley 2400 SourceMeter. The voltage measured at several places was approximately 8.7 mV. To convert this to a resistivity and conductivity we need to use some scaling factors. The website `https://www.ossila.com/pages/sheet-resistance-theory` references a paper at: `https://www.iiserkol.ac.in/~ph324/StudyMaterials/GeometricFactors4ProbeResistivity.PDF`, which provides the resistivity for a semi-infinite plane of finite thickness. Since our sample length and width (≈145 mm

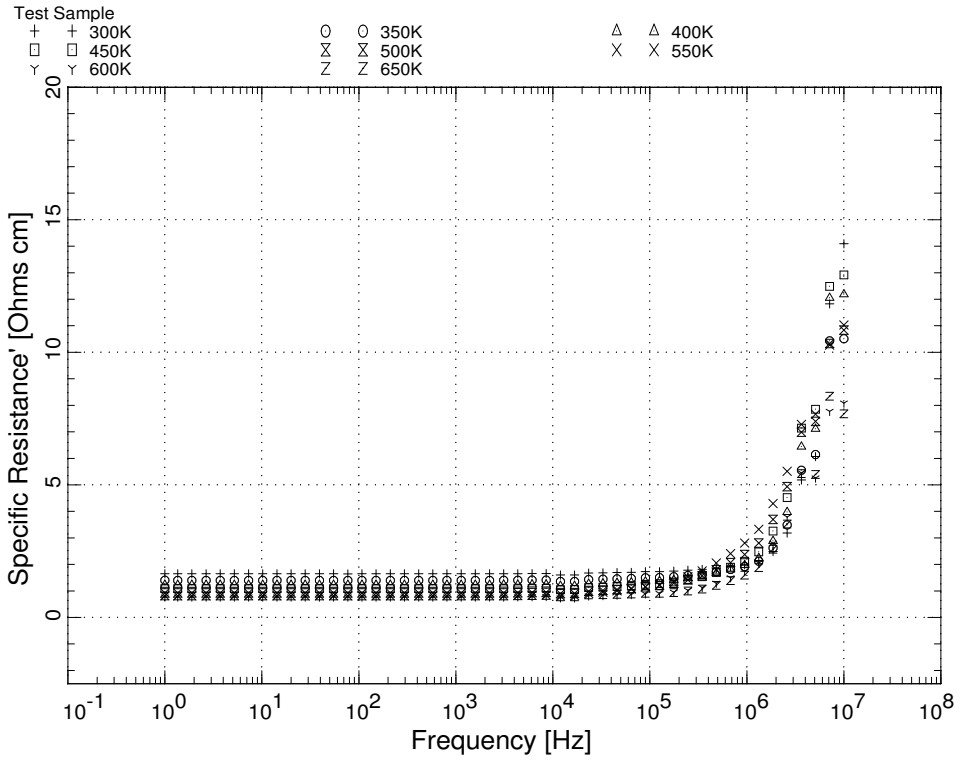

Figure 10. Resistivity of layer 2 as a function of frequency and temperature.

Figure 11. Photo showing the four-point system used to measure the resistivity of the charred AVCOAT at room temperature.

x 35 mm) are many times the probe tip spacing ($s = 1$ mm), this is a good approximation for our sample. The thickness of the charred layer is around $t = 4$ mm. The equation for resistivity on page 13 of the report is

$$\rho = G\frac{V}{I}, \tag{1}$$

where I is the constant current source between the outer probe points and V is the voltage read from the inner two probe tips. G is the scaling factor given by

$$G = 2\pi s T_1(t/s), \tag{2}$$

where $T_1(4/1) = 0.985$ according to the graph on page 14. Plugging all the numbers into the equation, we get $\rho = 0.00054\Omega$-m for the resistivity and $\sigma = 1860$ S/m for the conductivity. In the Novocontrol system measurements in the prior two sections the lowest resistivity of the charred AVCOAT was $\rho = 0.0164\Omega$-m which corresponds to a conductivity of $\sigma = 61$ S/m. So, the four-point measurement shows that the room temperature conductivity of the charred AVCOAT is actually 30.5 times higher than previously measured due to the errors associated with the contact resistances inherent in the Novocontrol measurement technique.

4.4 Results - Layer 3

Figure 12 shows photos of both sides of layer 3 of the charred AVCOAT. This layer shows a clear transition between the black charred outer region and the inner tan virgin AVCOAT.

Figure 13 shows the real relative permittivity of the material as a function of temperature. The permittivity seems to increase slightly with temperature. The knee that occurs at 650K may be due to a very low frequency relaxation, but it is also possible the material has deformed due to the heating and biased the measurement. The corresponding resistivity plot is shown in Figure 14 showing large decreases in resistivity as the temperature is increased.

4.5 Results - Layer 4

Figure 15 shows photos of both sides of layer 4 of the charred AVCOAT. This sample doesn't exhibit the black charring present in the first three layers but does have some darkening compared to virgin AVCOAT.

Figure 16 shows the real relative permittivity of the material as a function of temperature. The overall trend is for the permittivity to increase with temperature but decrease with frequency. Some variation to the trend is seen but this is likely related to the off-gassing and chemical changes the sample undergoes at the higher temperatures. The resistivity of the sample (shown in Figure 17) tends to decrease as the temperature increases at frequencies below 1 kHz. Above 1 kHz, the behavior varies probably due to the chemical changes occurring as the sample heats.

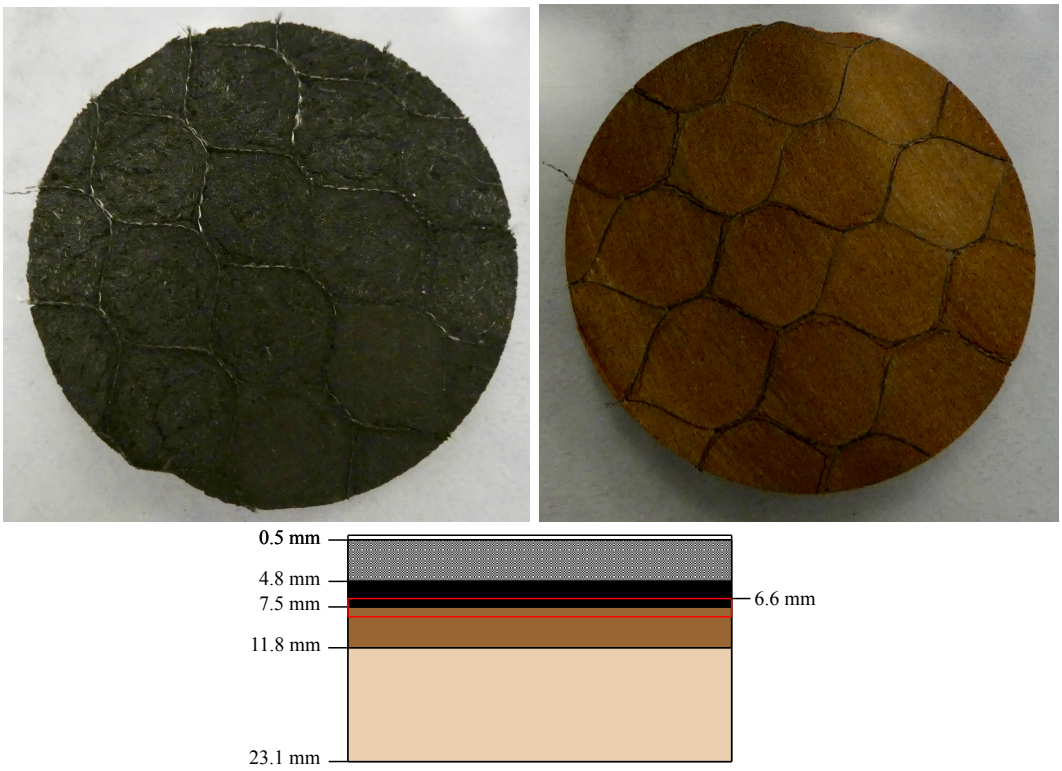

Figure 12. Photos showing both sides of a sample cut from layer 3 of a charred AVCOAT taken from a section of the analog heat shield for EFT-1. The sample is about 40 mm in diameter and 1.9 mm thick and shows a clear transition between the charred outer material and the virgin inner material. The diagram on the bottom shows the approximate location the sample is from within the cylindrical core (6.6 mm from original surface).

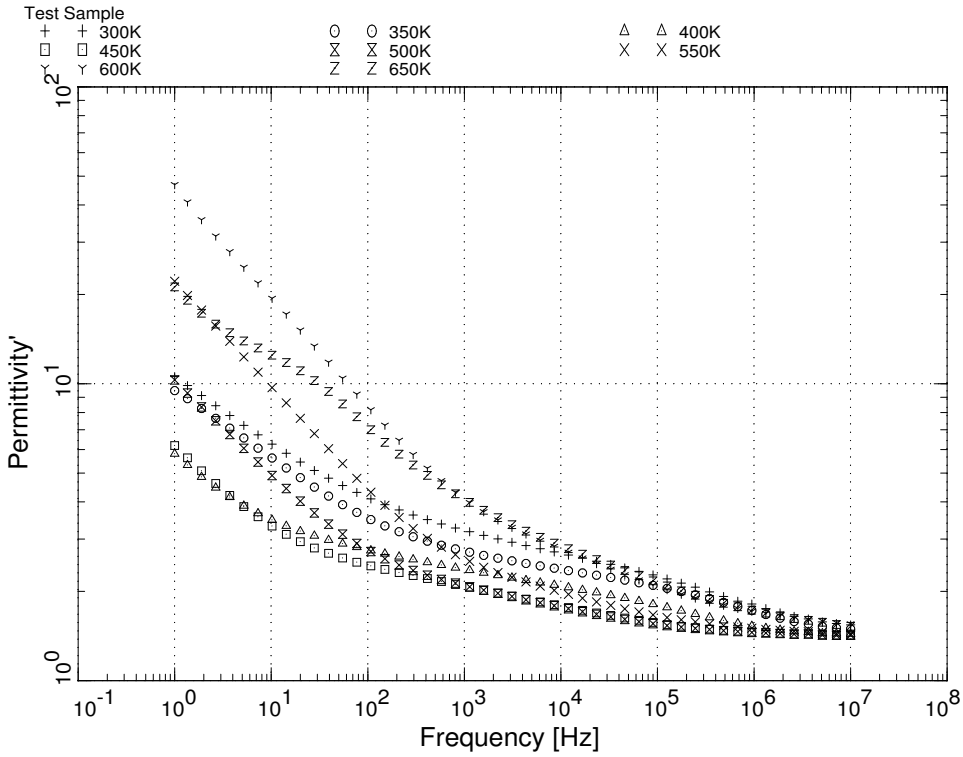

Figure 13. Real relative permittivity of layer 3 as a function of frequency and temperature.

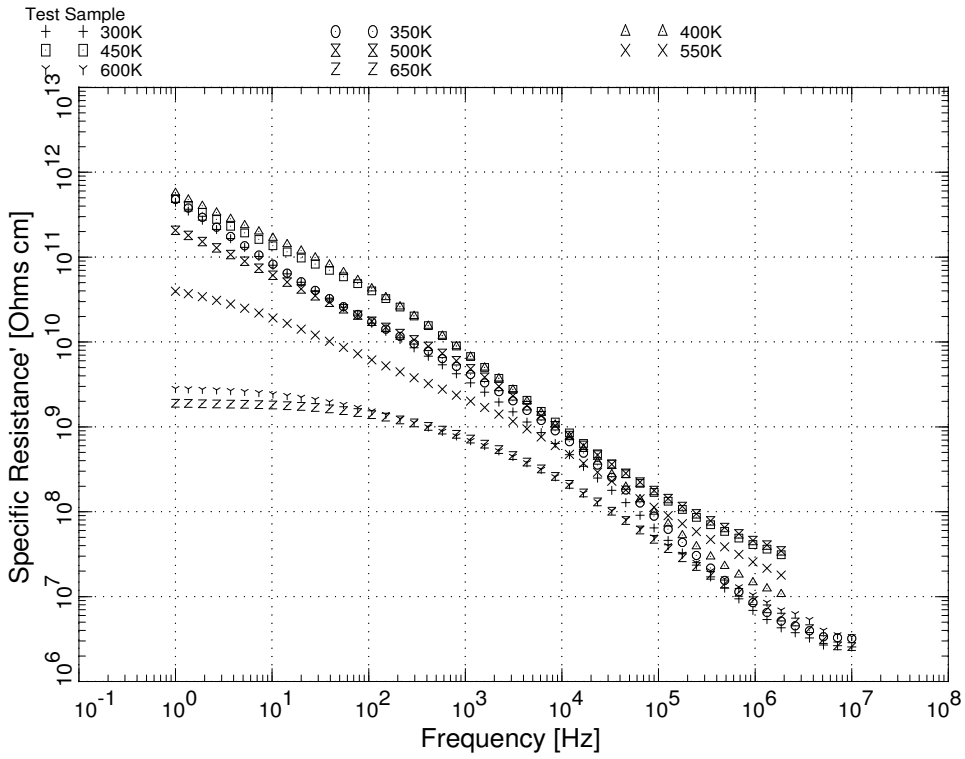

Figure 14. Resistivity of layer 3 as a function of frequency and temperature.

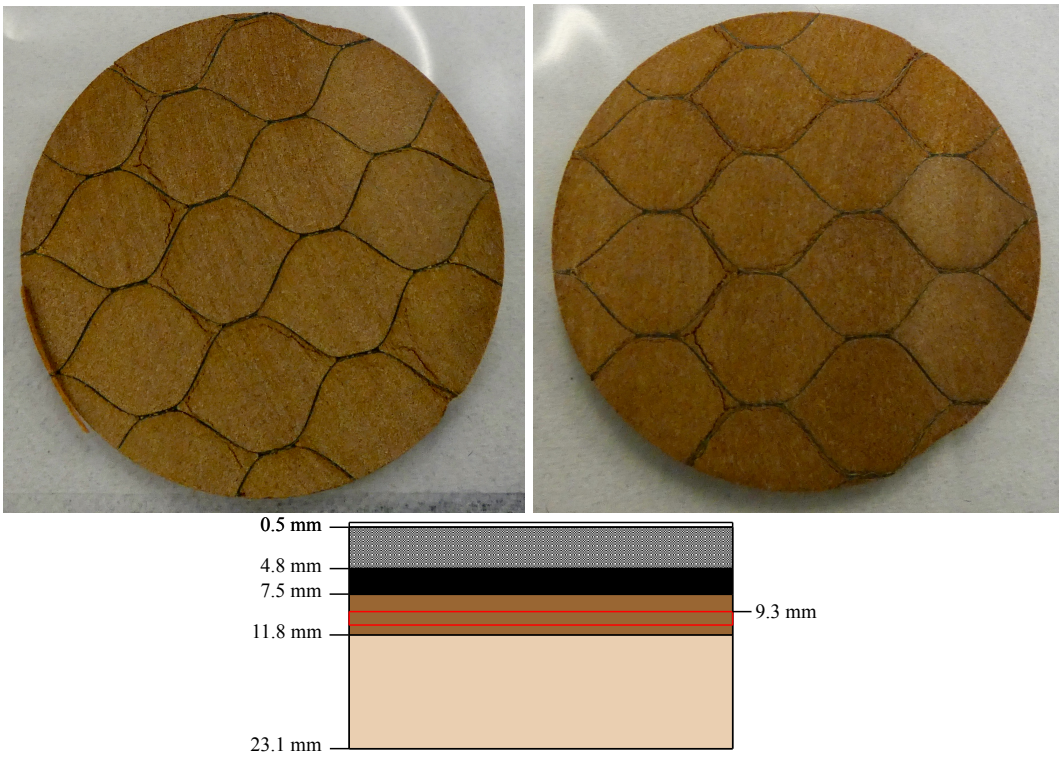

Figure 15. Photos showing both sides of a sample cut from layer 4 of charred AVCOAT taken from a section of the analog heat shield for EFT-1. The sample is about 40 mm in diameter and 1.4 mm thick. The diagram on the bottom shows the approximate location the sample is from within the cylindrical core (9.3 mm from original surface).

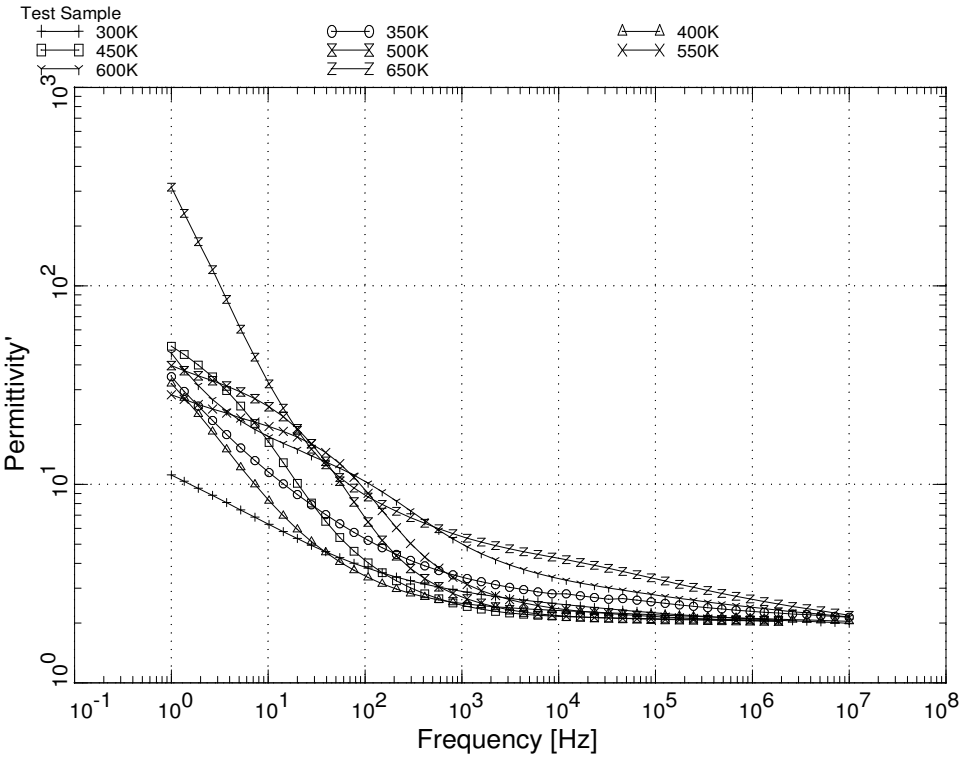

Figure 16. Real relative permittivity of layer 4 as a function of frequency and temperature.

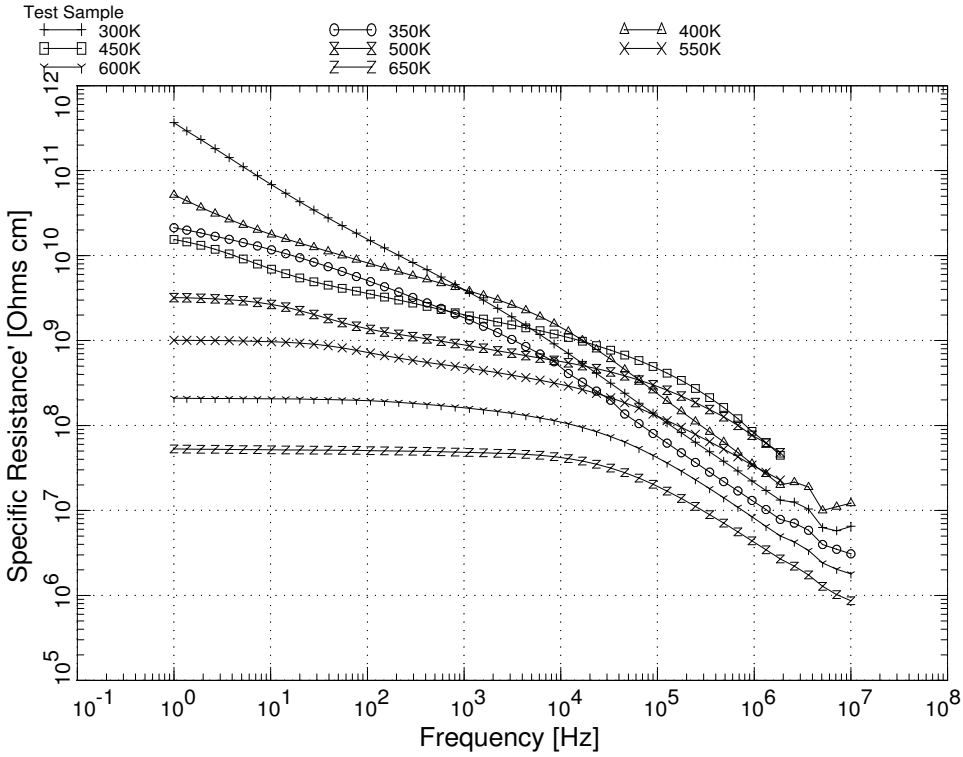

Figure 17. Resistivity of layer 4 as a function of frequency and temperature.

4.6 Results - Layer 5

Figure 18 shows photos of both sides of layer 5 of the charred AVCOAT. This sample doesn't exhibit the black charring present in the first three layers but does have some darkening compared to virgin AVCOAT.

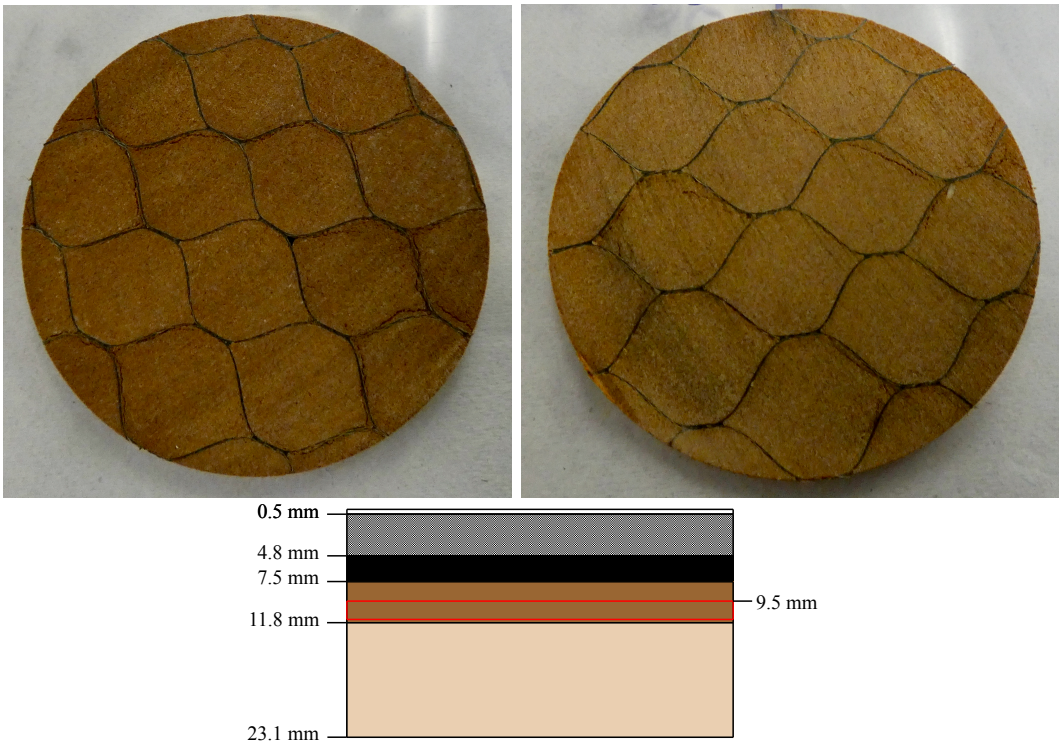

Figure 18. Photos showing both sides of a sample cut from layer 5 of charred AVCOAT taken from a section of the analog heat shield for EFT-1. The sample is about 40 mm in diameter and 1.9 mm thick. The diagram on the bottom shows the approximate location the sample is from within the cylindrical core (9.5 mm from original surface).

Figure 19 shows the real relative permittivity of the material as a function of temperature. The overall trend is for the permittivity to increase with temperature but decrease with frequency. Some variation to the trend is seen but this is likely related to the off-gassing and chemical changes the sample undergoes at the higher temperatures. The resistivity of the sample (shown in Figure 20) tends to decrease as the temperature increases at frequencies below 1 kHz. Above 1 kHz, the behavior varies probably due to the chemical changes occurring as the sample heats.

4.7 Results - Layer 6

Figure 21 shows photos of both sides of layer 6 of the charred AVCOAT. This sample doesn't exhibit any darkening and appears like virgin AVCOAT.

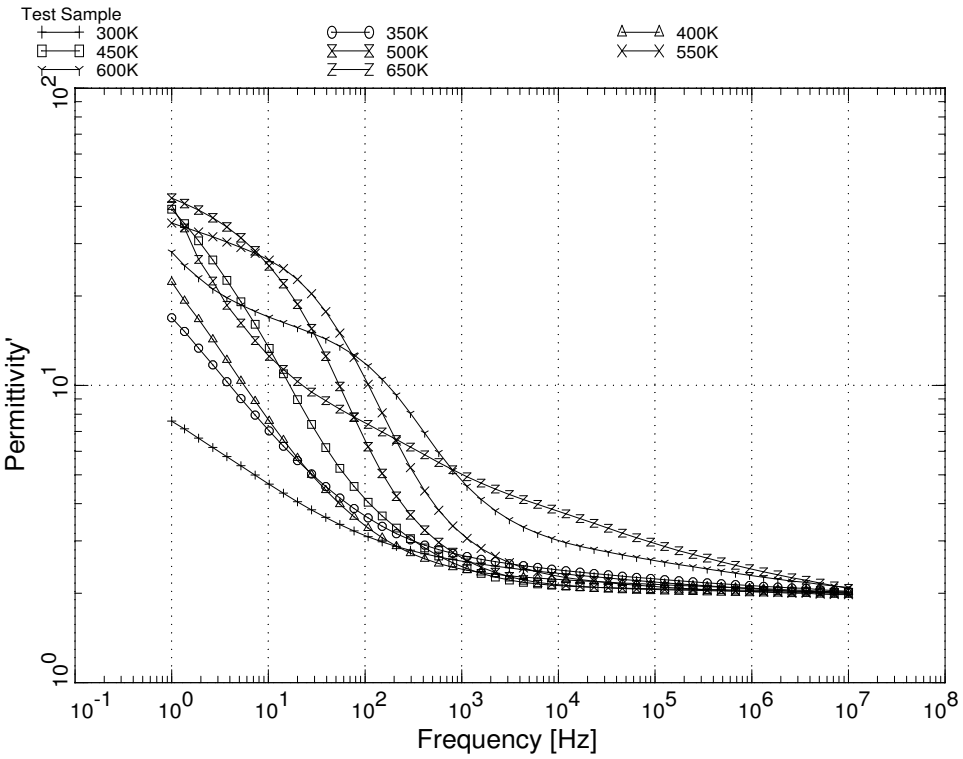

Figure 19. Real relative permittivity of layer 5 as a function of frequency and temperature.

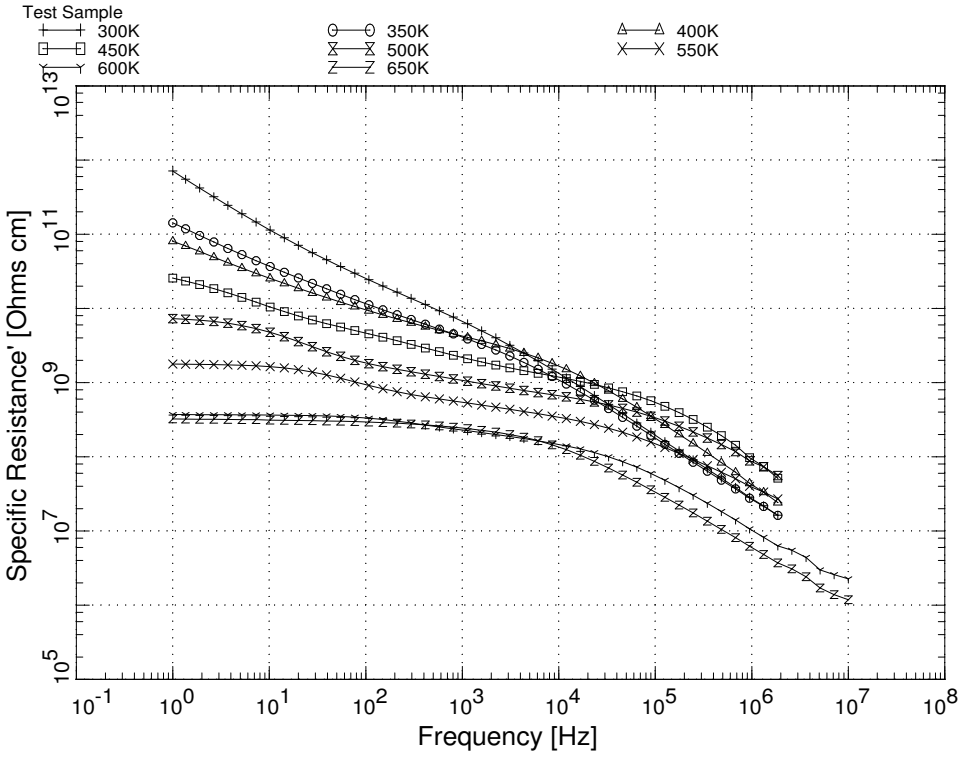

Figure 20. Resistivity of layer 5 as a function of frequency and temperature.

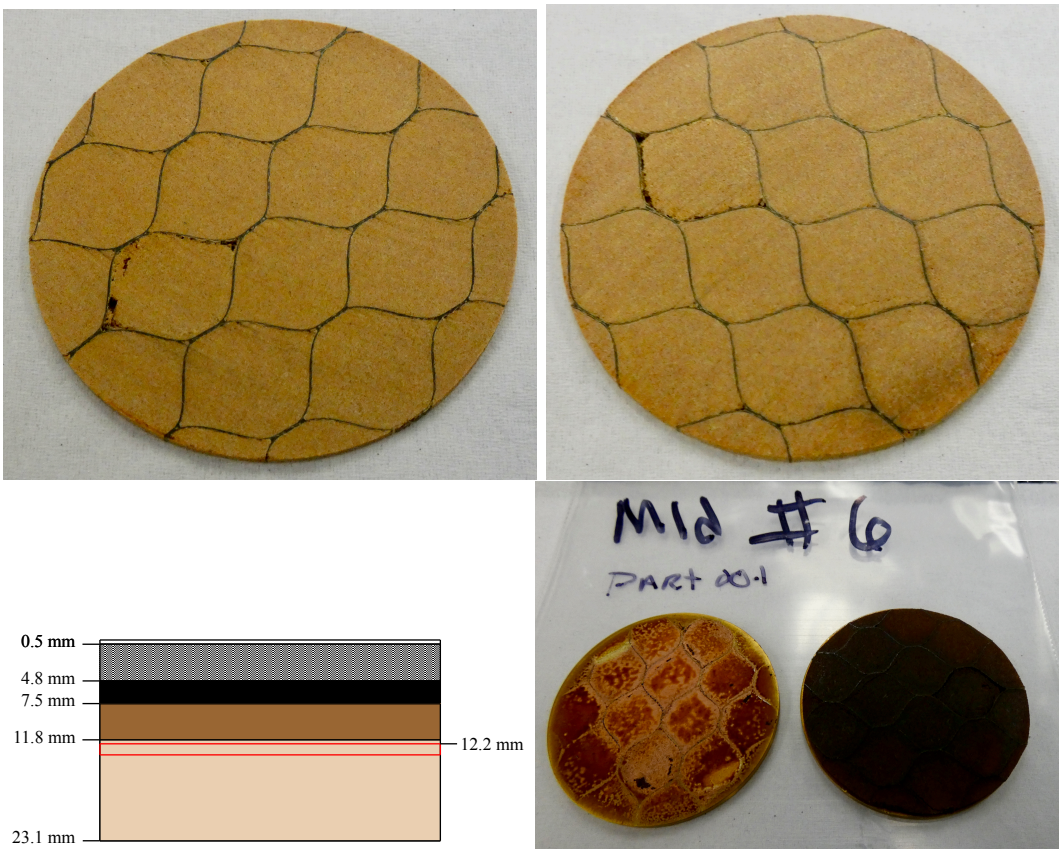

Figure 21. Photos showing both sides of a sample cut from layer 6 of charred AVCOAT taken from a section of the analog heat shield for EFT-1. The sample is about 40 mm in diameter and 1.3 mm thick. The diagram on the bottom left shows the approximate location the sample is from within the cylindrical core (12.2 mm from original surface). The photo in the lower right shows residue stuck to one of the test electrodes on the left and the blackened sample after testing on the right.

Figure 22 shows the real relative permittivity of the material as a function of temperature. The overall trend is for the permittivity to increase with temperature but decrease with frequency up until 450K. Above this temperature, the peak permittivity begins to decrease and is likely related to the off-gassing and chemical changes the sample undergoes at the higher temperatures. The resistivity of the sample (shown in Figure 23) tends to decrease as the temperature increases to 450K at frequencies below 100 Hz. The resistivity then increases at 500K as the sample begins undergoing chemical changes and then continues to decrease as the temperature is further increased. Above 100 Hz, the behavior varies probably due to the chemical changes occurring as the sample heats.

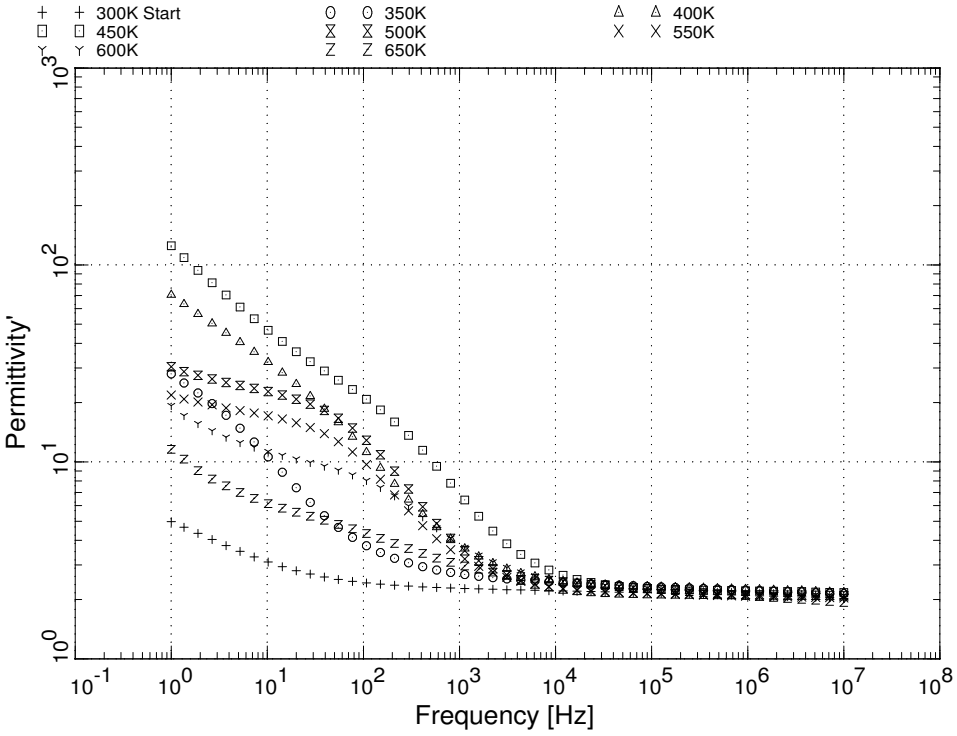

Figure 22. Real relative permittivity of layer 6 as a function of frequency and temperature.

4.8 Results - Layer 7

Figure 24 shows photos of both sides of layer 7 of the charred AVCOAT. This sample doesn't exhibit any darkening and appears like virgin AVCOAT.

Figure 25 shows the real relative permittivity of the material as a function of temperature. The overall trend is for the permittivity to increase with temperature but decrease with frequency up until 450K. Above this temperature, the peak permittivity begins to decrease and is likely related to the off-gassing and chemical changes the sample undergoes at the higher temperatures. The resistivity of the

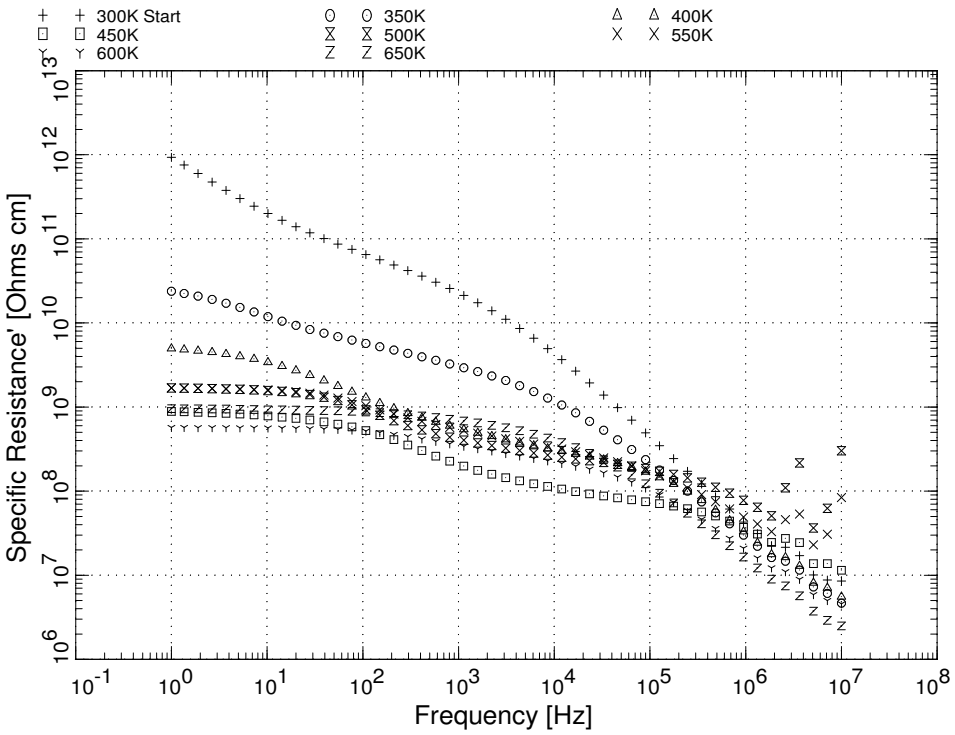

Figure 23. Resistivity of layer 6 as a function of frequency and temperature.

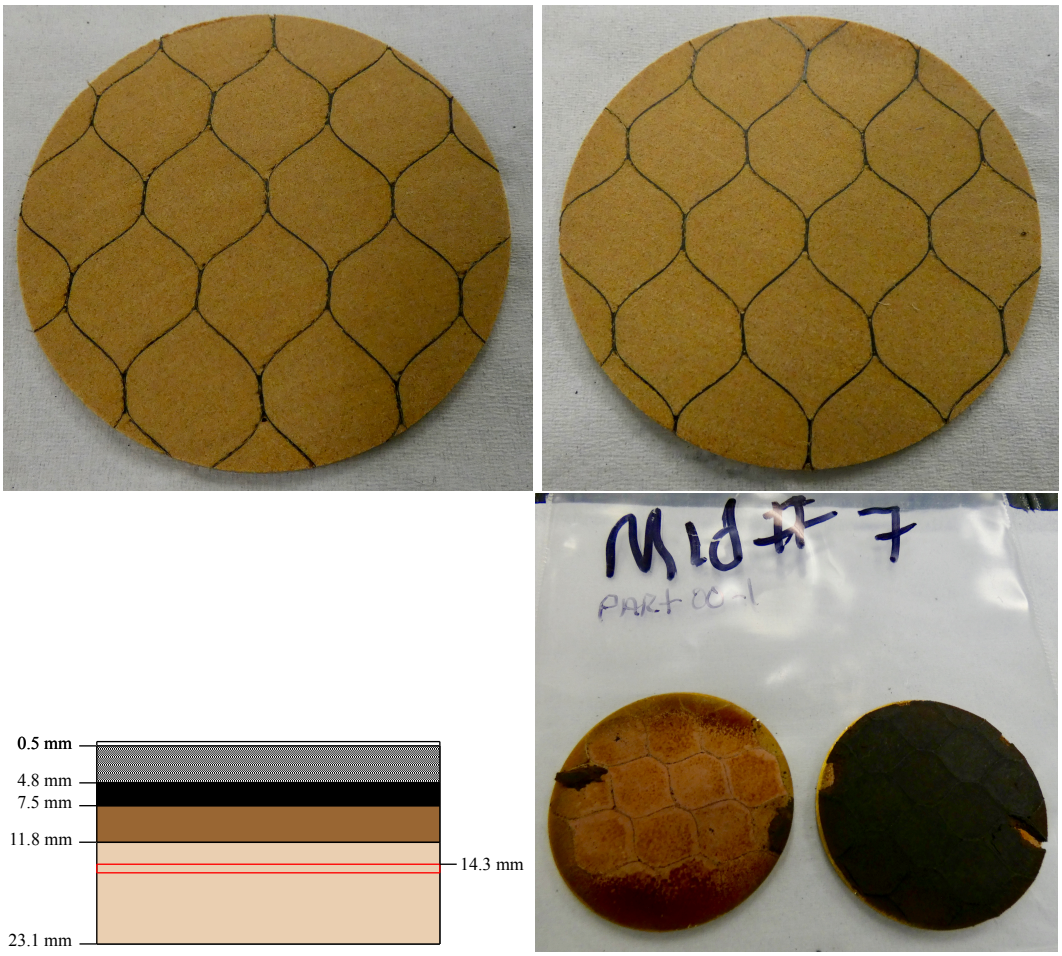

Figure 24. Photos showing both sides of a sample cut from layer 7 of charred AVCOAT taken from a section of the analog heat shield for EFT-1. The sample is about 40 mm in diameter and 1.0 mm thick. The diagram on the bottom left shows the approximate location the sample is from within the cylindrical core (14.3 mm from original surface). The photo in the lower right shows residue stuck to one of the test electrodes on the left and the blackened sam

sample (shown in Figure 26) tends to decrease as the temperature increases to 450K at frequencies below 1 kHz. The resistivity then increases at 500K as the sample begins undergoing chemical changes and then continues to decrease as the temperature is further increased. Above 1 kHz, the behavior varies probably due to the chemical changes occurring as the sample heats.

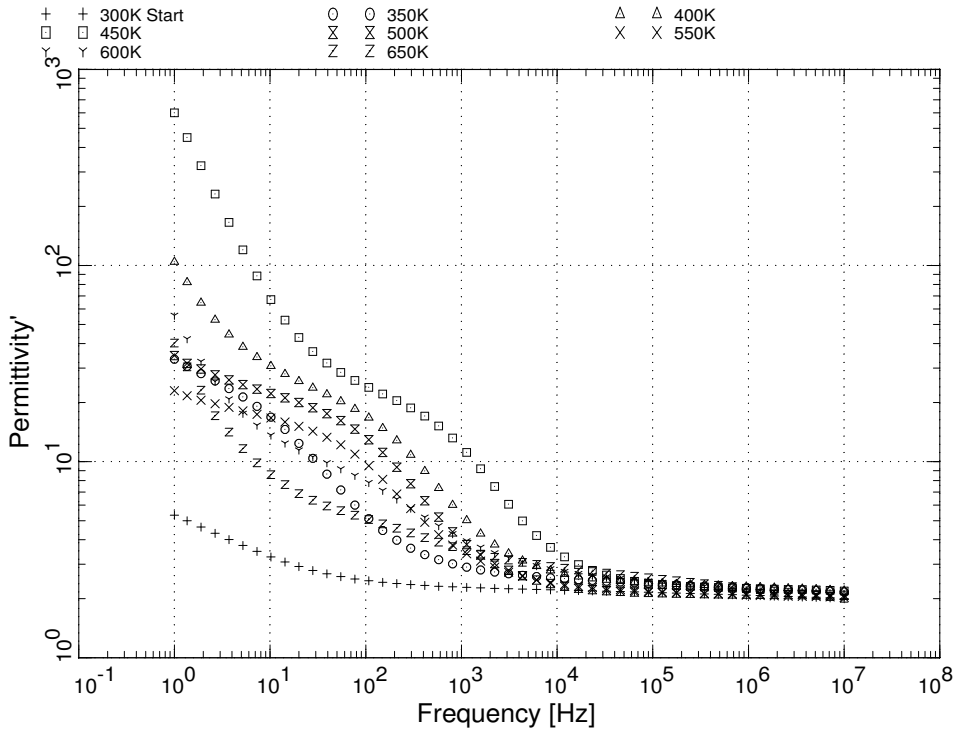

Figure 25. Real relative permittivity of layer 7 as a function of frequency and temperature.

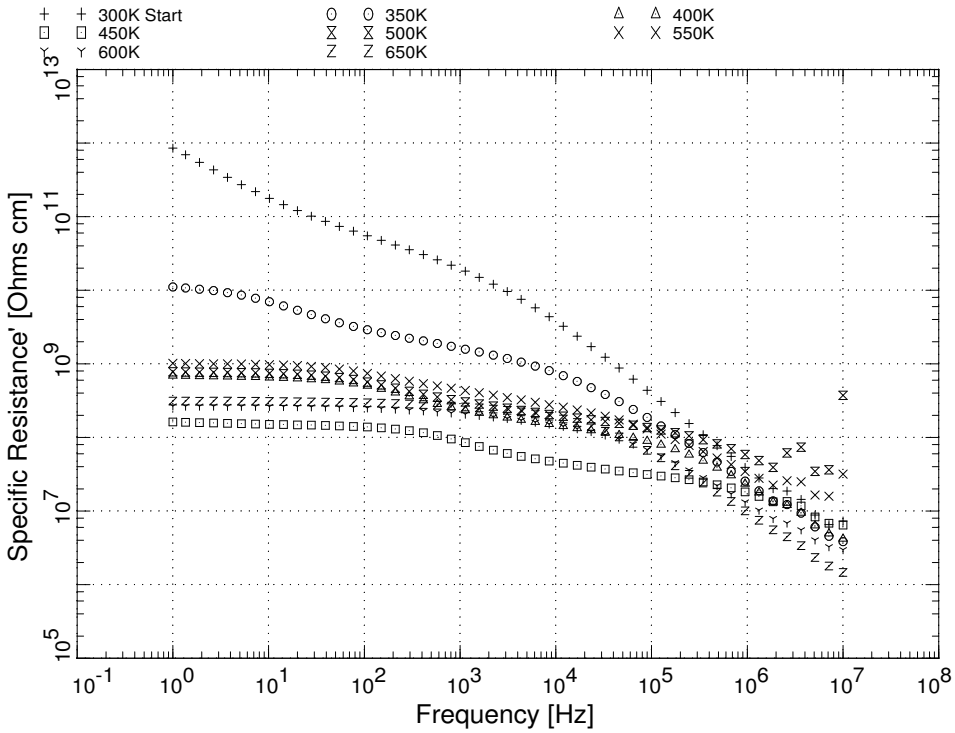

Figure 26. Resistivity of layer 7as a function of frequency and temperature.

4.9 Electrical Properties at Fixed Temperatures

Figures 27, 28, 29, 30 , 31 , 32 , 33 , and 34 are provided to give an alternate method of looking at the data. They show the electrical properties at fixed temperatures as a function of layer and frequency. The real permittivity for layers 1 and 2 is not shown since these samples are conductive and not accurately measured by our system. These layers can be considered to have a real relative permittivity of 1. The imaginary portion of the permittivity is proportional to the conductivity and inversely proportional to the resistivity, so those values were measurable and are provided for layers 1 and 2 in the resistivity figures.

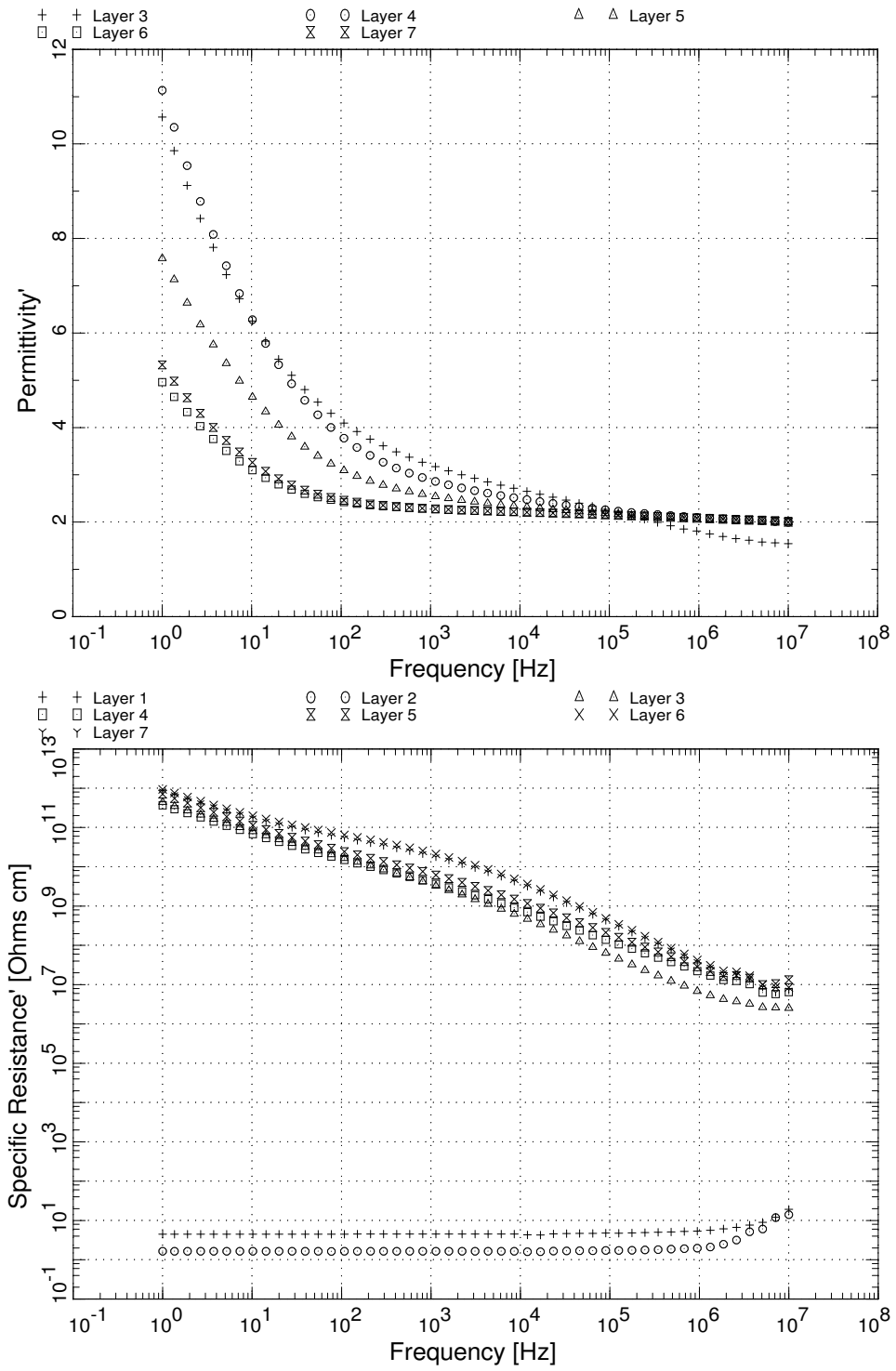

Figure 27. The upper plot shows the real relative permittivity for each layer at 300K while the bottom layer shows the resistivity for that same temperature.

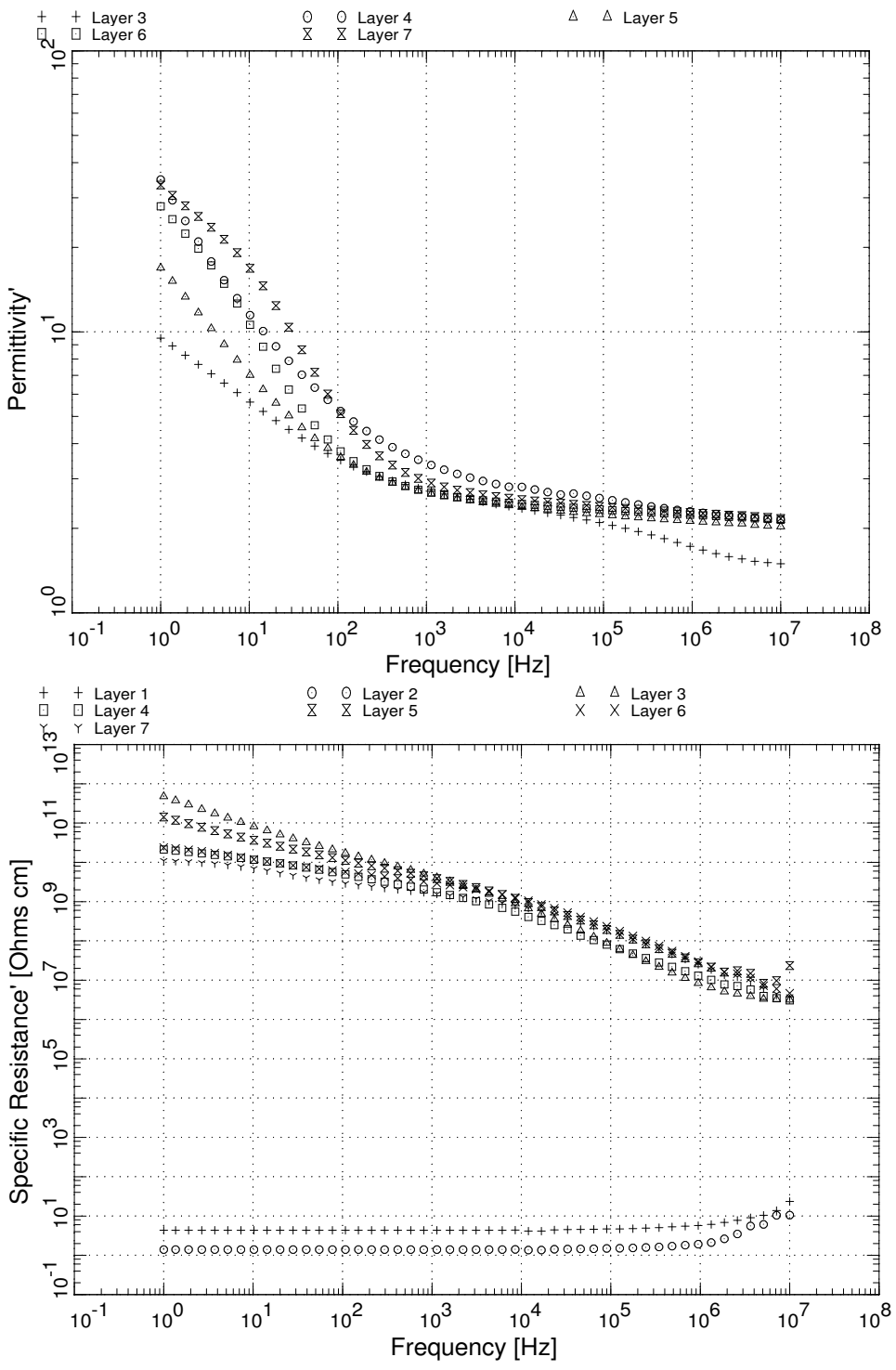

Figure 28. The upper plot shows the real relative permittivity for each layer at 350K while the bottom layer shows the resistivity for that same temperature.

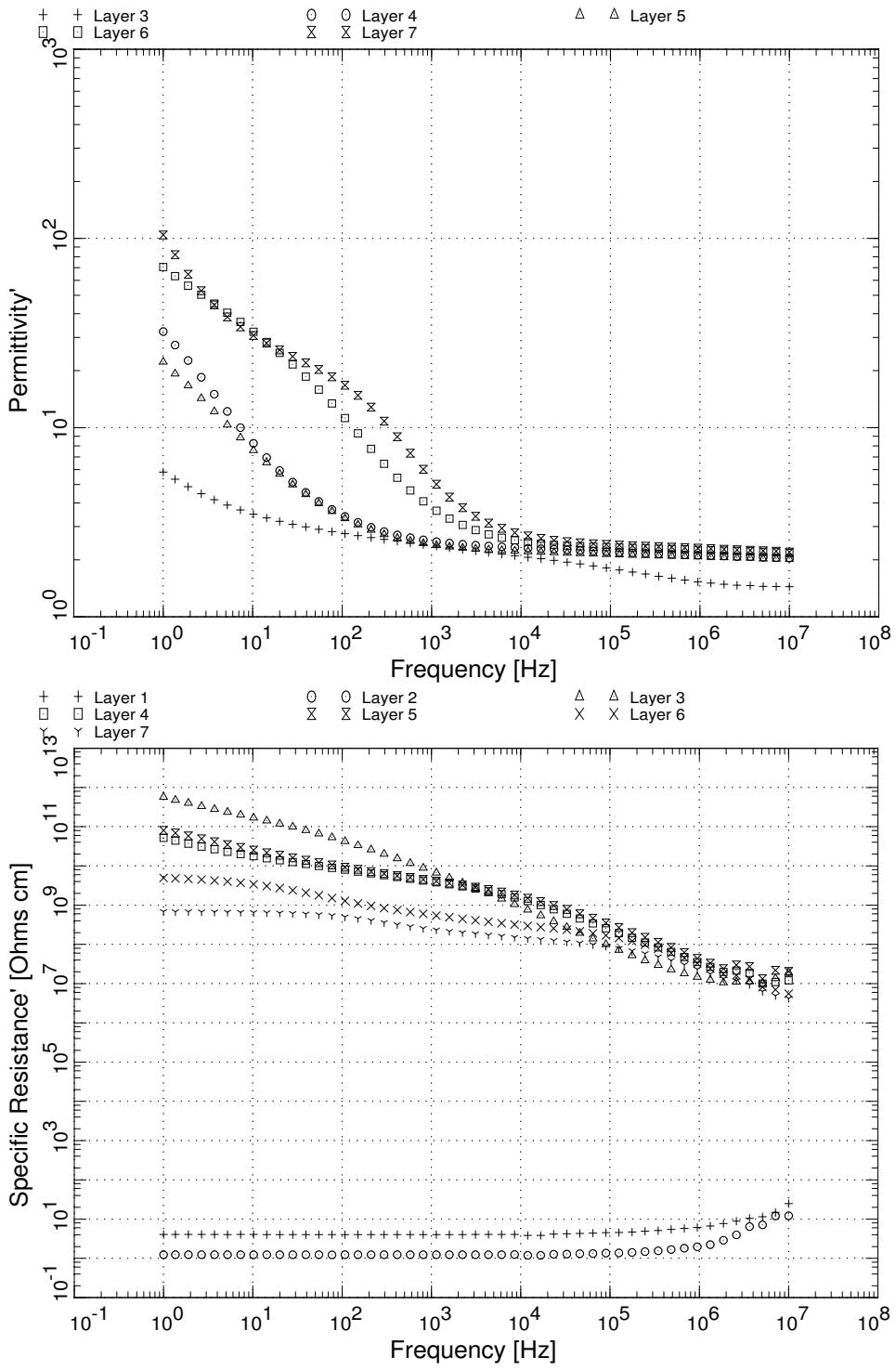

Figure 29. The upper plot shows the real relative permittivity for each layer at 400K while the bottom layer shows the resistivity for that same temperature.

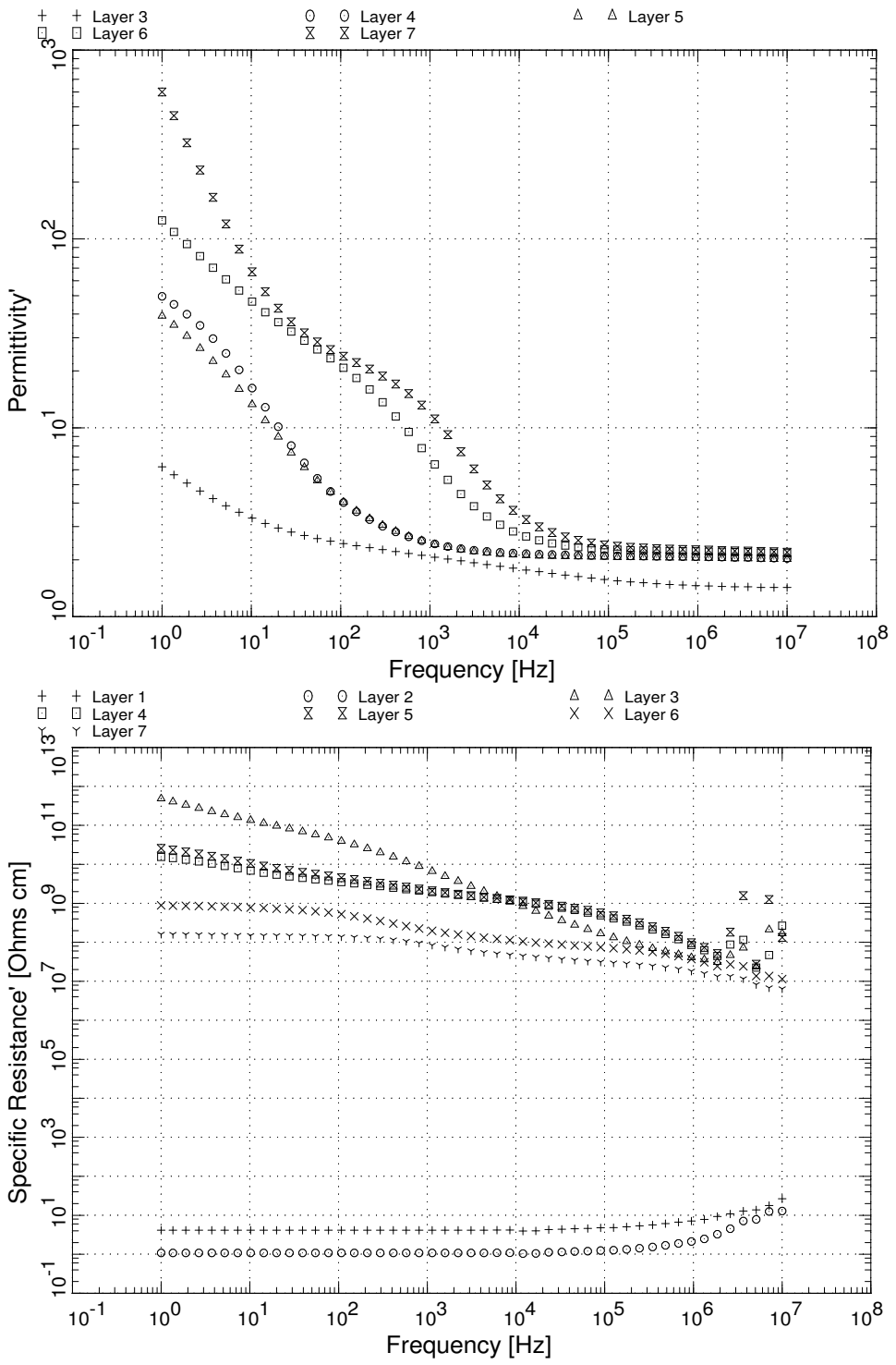

Figure 30. The upper plot shows the real relative permittivity for each layer at 450K while the bottom layer shows the resistivity for that same temperature.

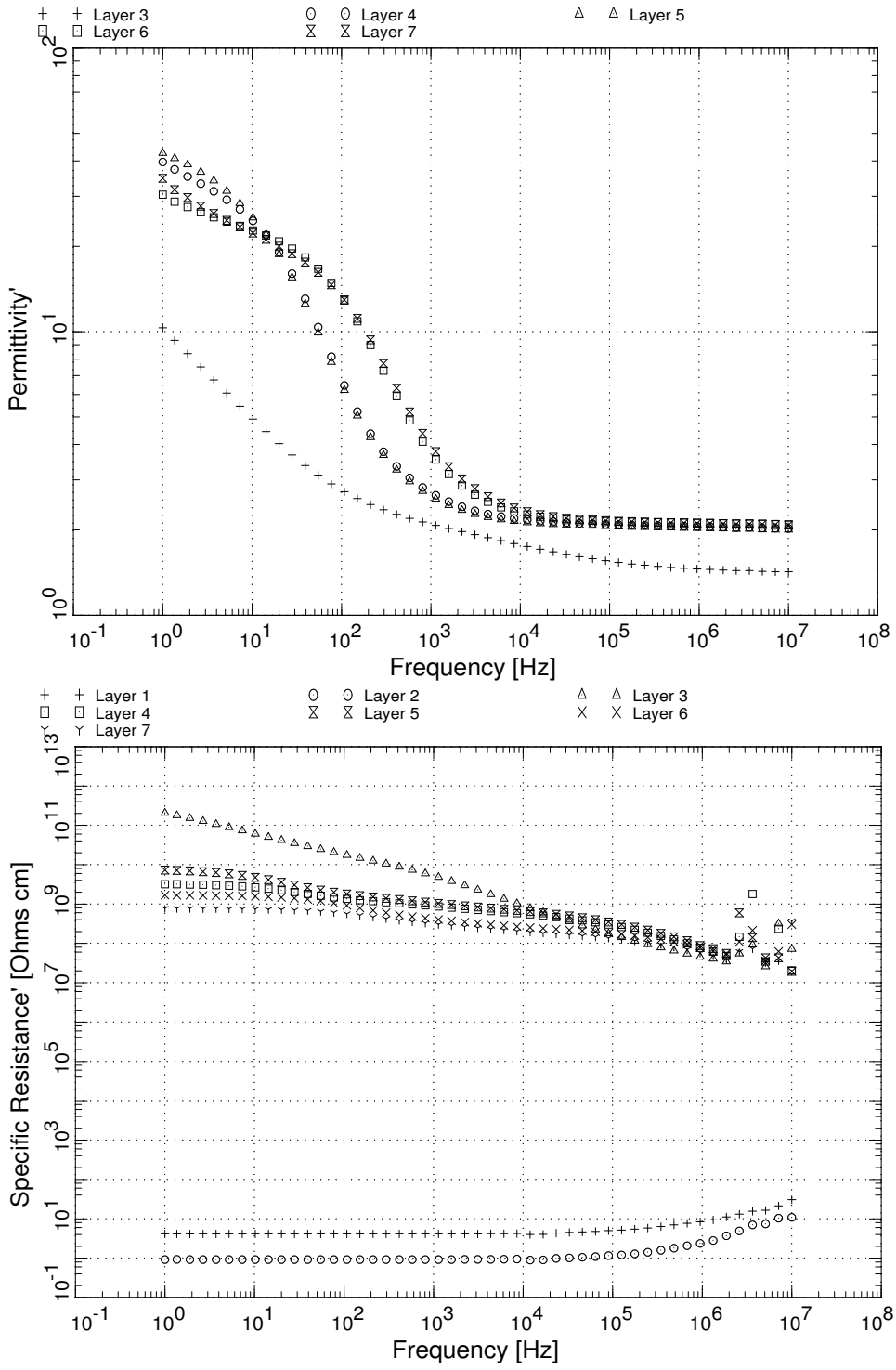

Figure 31. The upper plot shows the real relative permittivity for each layer at 500K while the bottom layer shows the resistivity for that same temperature.

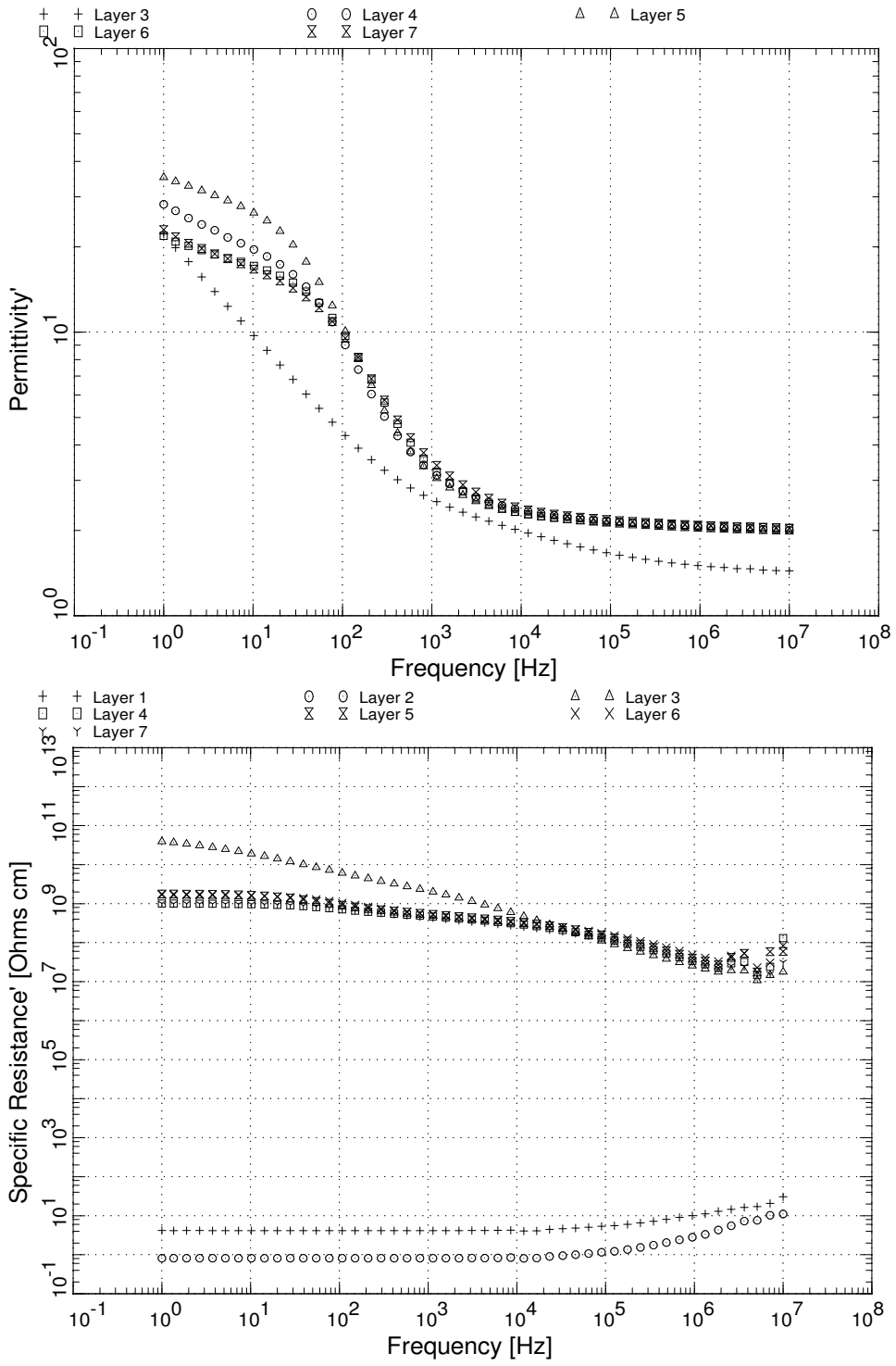

Figure 32. The upper plot shows the real relative permittivity for each layer at 550K while the bottom layer shows the resistivity for that same temperature.

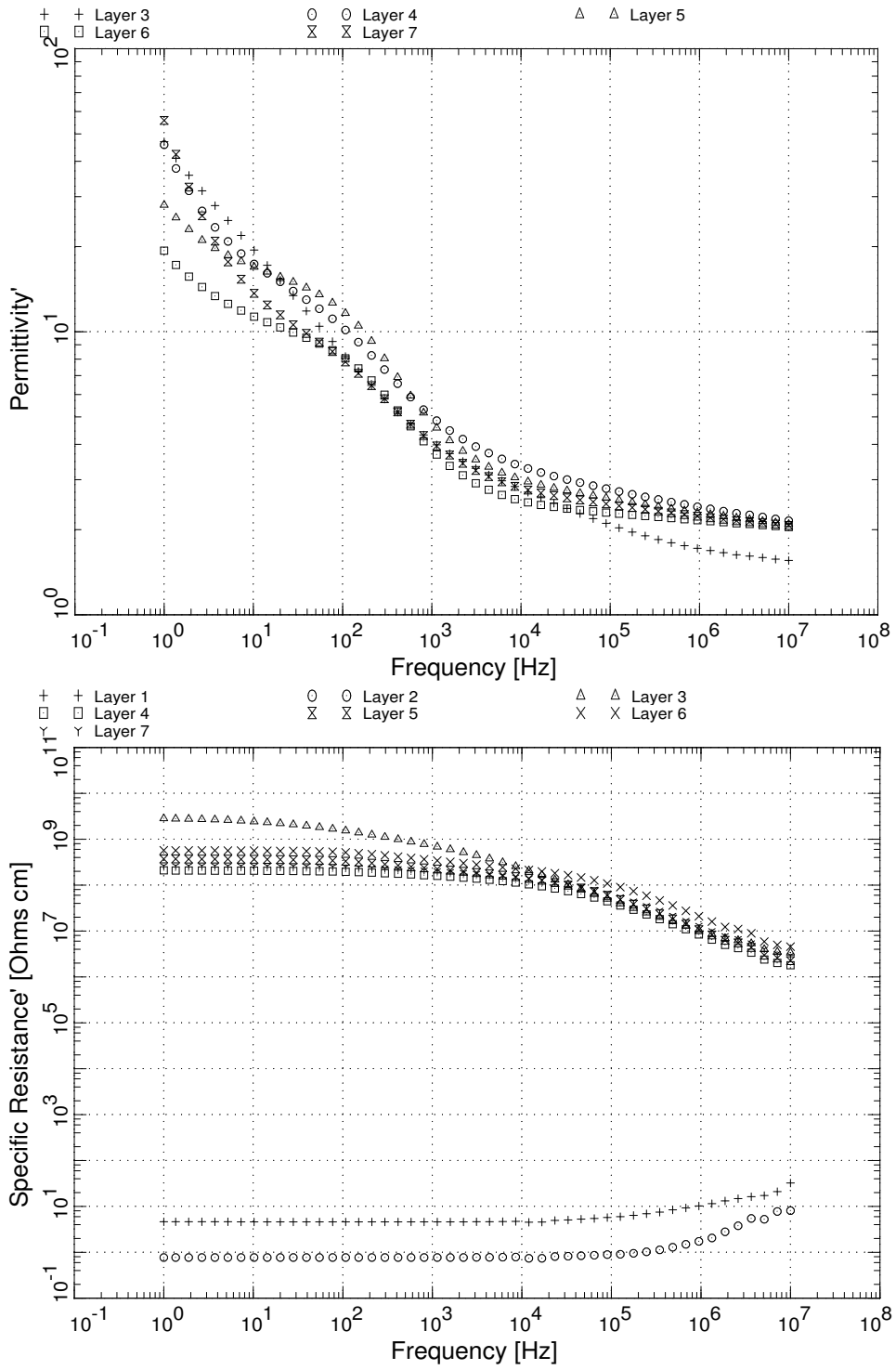

Figure 33. The upper plot shows the real relative permittivity for each layer at 600K while the bottom layer shows the resistivity for that same temperature.

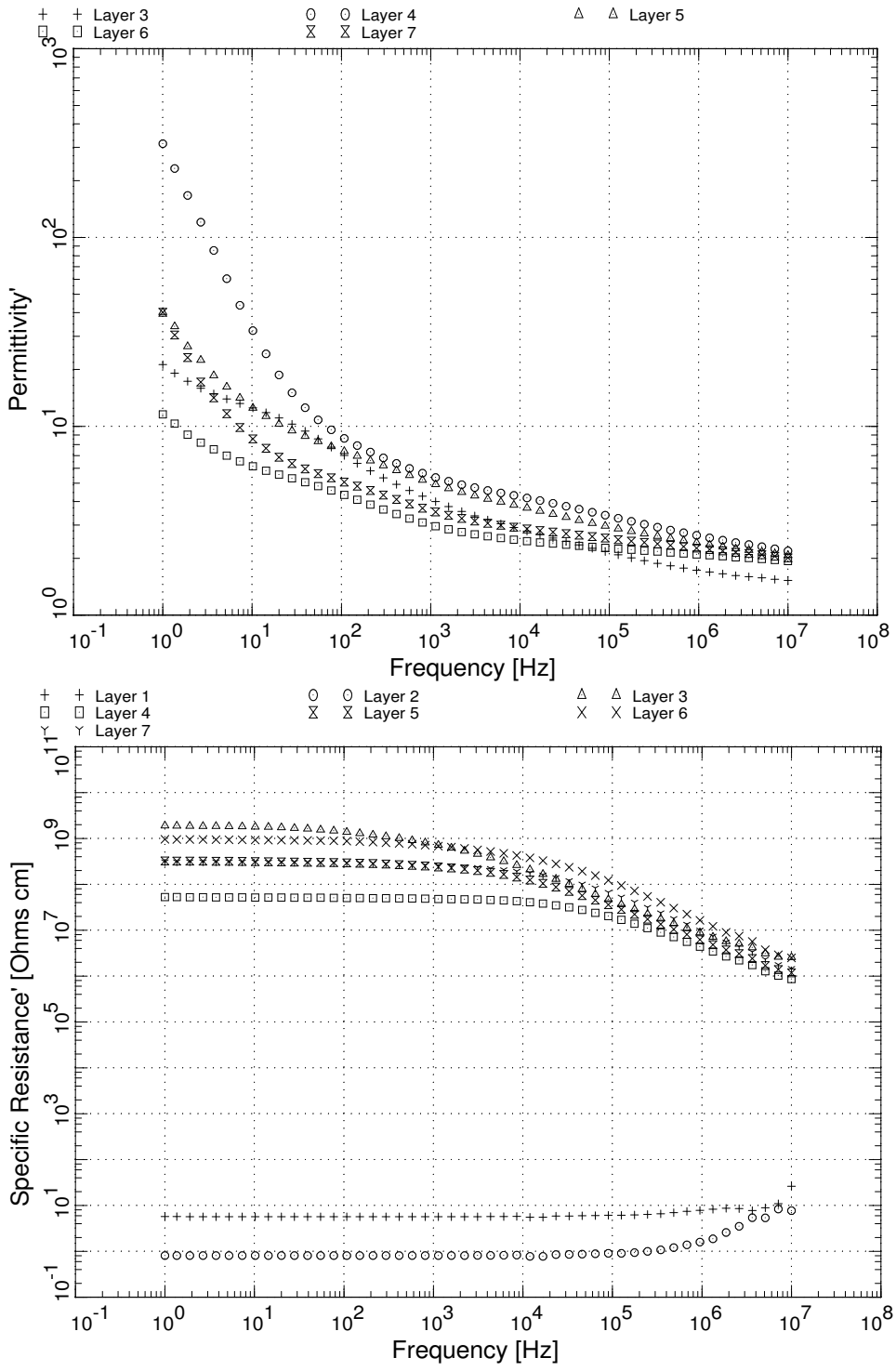

Figure 34. The upper plot shows the real relative permittivity for each layer at 650K while the bottom layer shows the resistivity for that same temperature.

5 Temperature and Frequency Dependent Electrical Properties of Reaction Cured Glass (RCG) Coating from Shuttle High-Temperature Reusable Insulation (HRSI)

A sample of Shuttle tile flown on early Challenger missions was cut on the side to remove the coating. The glass fibers were sanded until nothing but the black coating showed. The sample was then placed between a pair of 20 mm diameter auxiliary electrodes and measured with a Novocontrol Concept 40 Broadband Dielectric Spectroscopy system at Kennedy Space Center. A photo of each side appears in Figure 35 below.

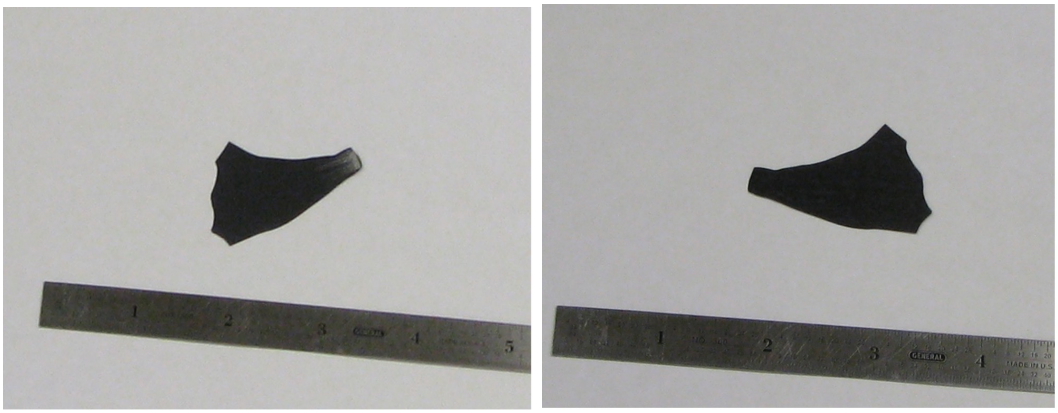

Figure 35. Photos showing both sides of a Shuttle tile RCG coating removed from the side of an early Challenger tile.

The dielectric spectroscopy system measures the complex capacitance of the sample using a known capacitor geometry and then derives the material properties. Typically, an insulator is represented as a complex permittivity with the real portion representing the polarizability of the material and the imaginary portion is associated with the loss mechanism (i.e, conductivity/ resistivity). This sample was measured over a frequency range from 1 Hz-10 MHz and a temperature range of 300K to 650K in steps of 50K.

For the purposes of this report, the data shown below in Figure 36 is the real portion of the permittivity with the permittivity of free space removed (also known as the relative permittivity or the dielectric constant). Figure 37 is the specific resistance of the material which is computed from the imaginary portion of the permittivity measurement. Both plots show the data for the sample starting at room temperature followed by the data at elevated temperatures and then ending at room temperature. This is done to see if moisture in the sample bakes out and changes the measurements in any way. In this case, the measurements for the starting temperature of 300K and the ending temperature of 300K appear to be similar. The rise in permittivity below 1 kHz, in the 500K-650K curves appears to be due to a sub-1 Hertz relaxation in the tile coating that begins to show up at higher

frequencies as the temperature is raised. There are corresponding slope changes in the specific resistance (although not as pronounced) at similar frequencies due to this phenomenon.

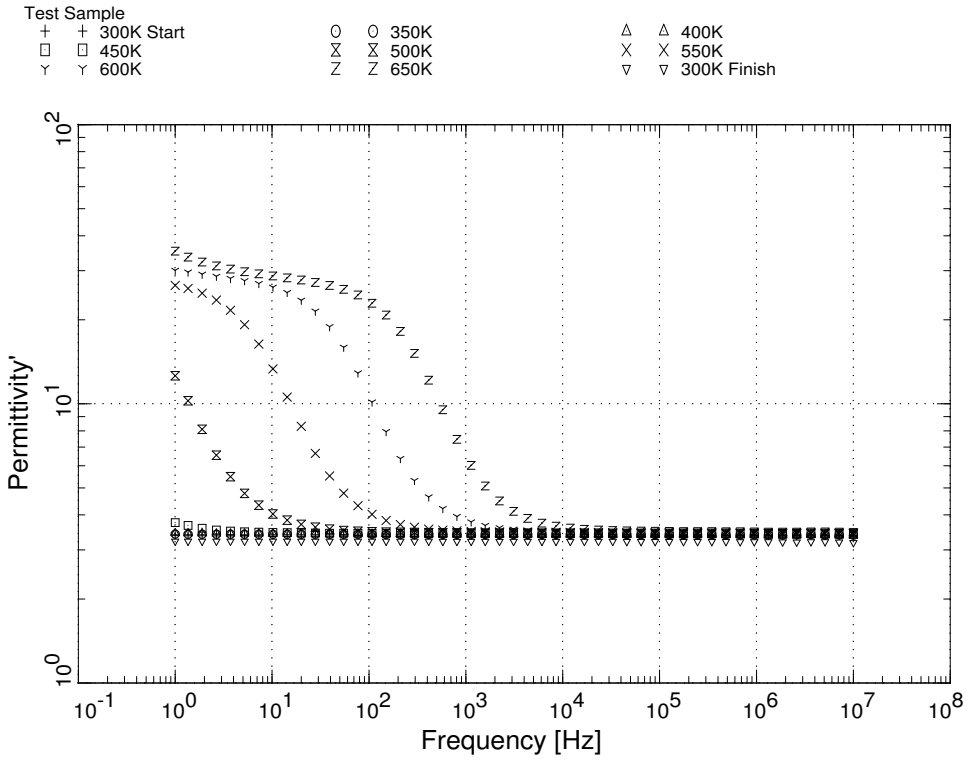

Figure 36. Permittivity of Shuttle thermal protection tile RCG coating as a function of frequency and temperature

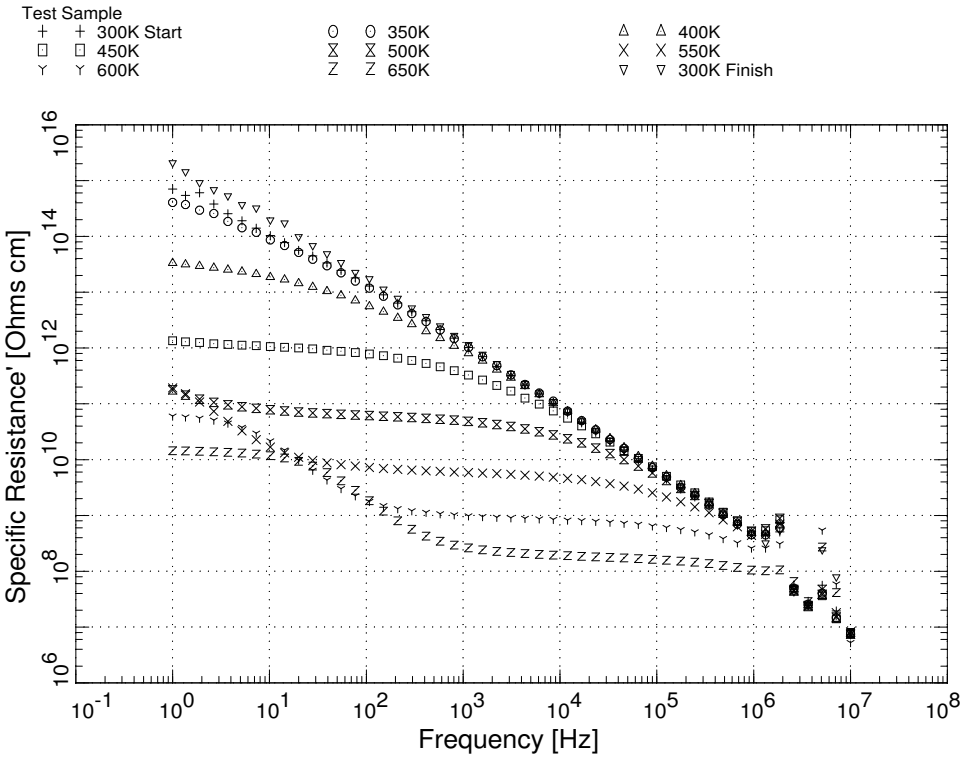

Figure 37. Resistivity of Shuttle thermal protection tile RCG coating as a function of frequency and temperature.

6 Temperature and Frequency Dependent Electrical Properties of Aluminum Enhanced Thermal Barrier (AETB) Coating from Shuttle High-Temperature Reusable Insulation (HRSI)

The outer coating was cut from a sample AETB tile and made into several test samples of which two were tested. Each sample was then placed between a pair of auxiliary electrodes and measured with a Novocontrol Concept 40 Broadband Dielectric Spectroscopy system at Kennedy Space Center. The dielectric spectroscopy system measures the complex capacitance of the sample using a known capacitor geometry and then derives the material properties. Typically, an insulator is represented as a complex permittivity with the real portion representing the polarizability of the material and the imaginary portion is associated with the loss mechanism (i.e, conductivity/ resistivity). These samples were measured over a frequency range from 1 Hz-10 MHz and a temperature range of 300K to 650K in steps of 50K.

6.1 Sample 1 Results

The first sample is shown in Figure 38 below.

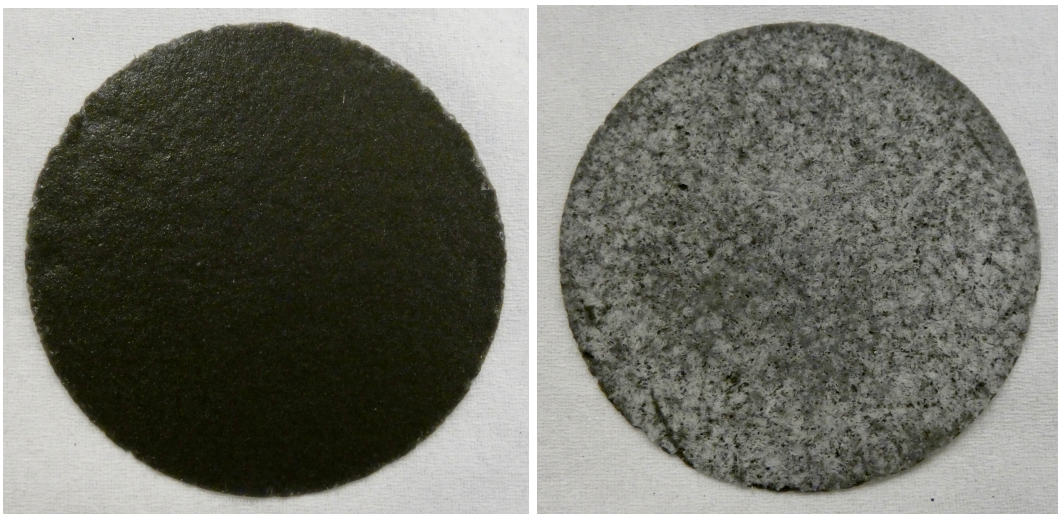

Figure 38. Photos showing both sides of the outer coating taken from an AETB tile. The outer surface is on the left. The inner surface (right) still show some of the white coloration of the insulating glass fibers. This sample is 40 mm in diameter and 0.5 mm thick.

Figure 39 shows the temperature ramp used while measuring the electrical properties. The set point is represented in red while the actual sample temperature appears in black.

For the purposes of this report, the data shown below in Figure 40 is the real

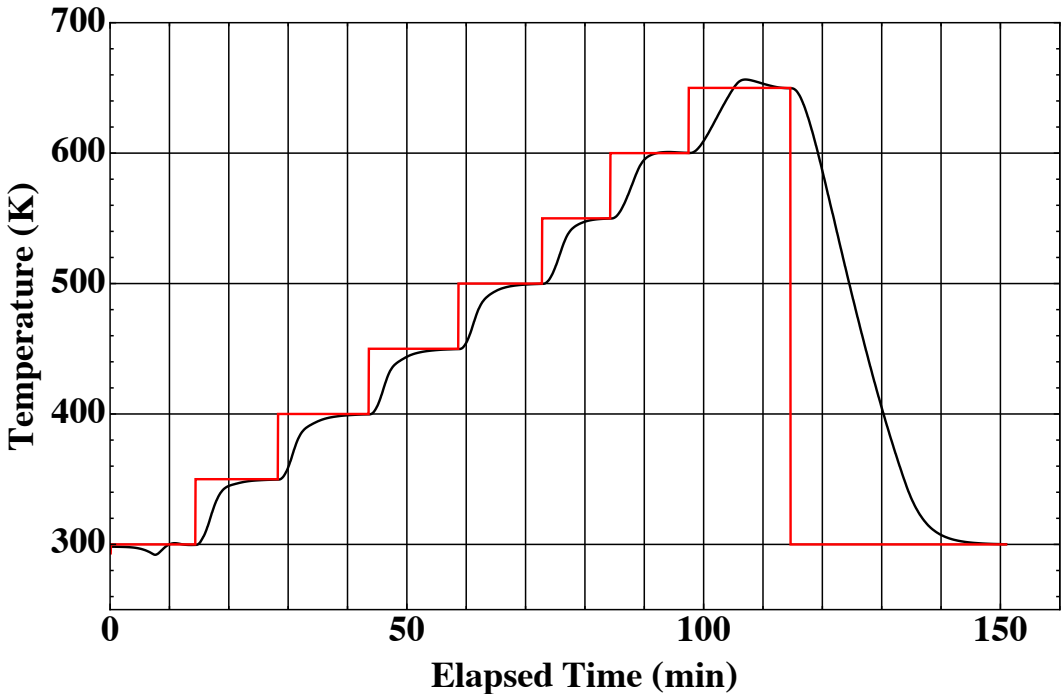

Figure 39. Temperature versus time profile for testing sample 1. The red curve shows the set temperatures, while the black shows the actual sample temperature.

portion of the permittivity with the permittivity of free space removed (also known as the relative permittivity or the dielectric constant). Figure 4 is the specific resistance of the material which is computed from the imaginary portion of the permittivity measurement. The rise in permittivity below 1 kHz, in the 500K-650K curves appears to be due to a sub-1 Hertz relaxation in the tile coating that begins to show up at higher frequencies as the temperature is raised. There are corresponding slope changes in the specific resistance (although not as pronounced) at similar frequencies due to this phenomenon.

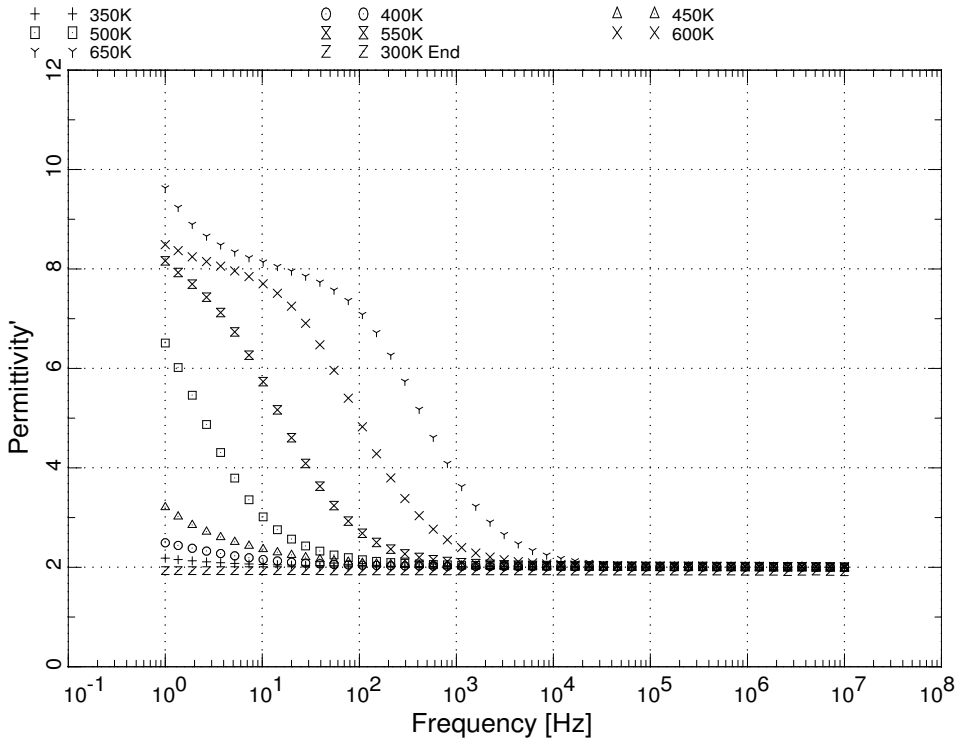

Figure 40. Permittivity of AETB tile coating of sample 1 as a function of frequency and temperature.

6.2 Sample 2 Results

The 2nd sample is shown in Figure 42 below. The 40 mm diameter sample broke in half during machining so one half of the sample was used with 20 mm diameter electrodes. The photos show the size of the sample, but the sample broke further upon removal from the test cell (cracks present in the photos.

Figure 43 shows the temperature ramp used while measuring the electrical properties. The set point is represented in red while the actual sample temperature appears in black.

The data shown below in Figure 44 is the real relative permittivity of sample 2. Figure 45 is the specific resistance of the material which is computed from the

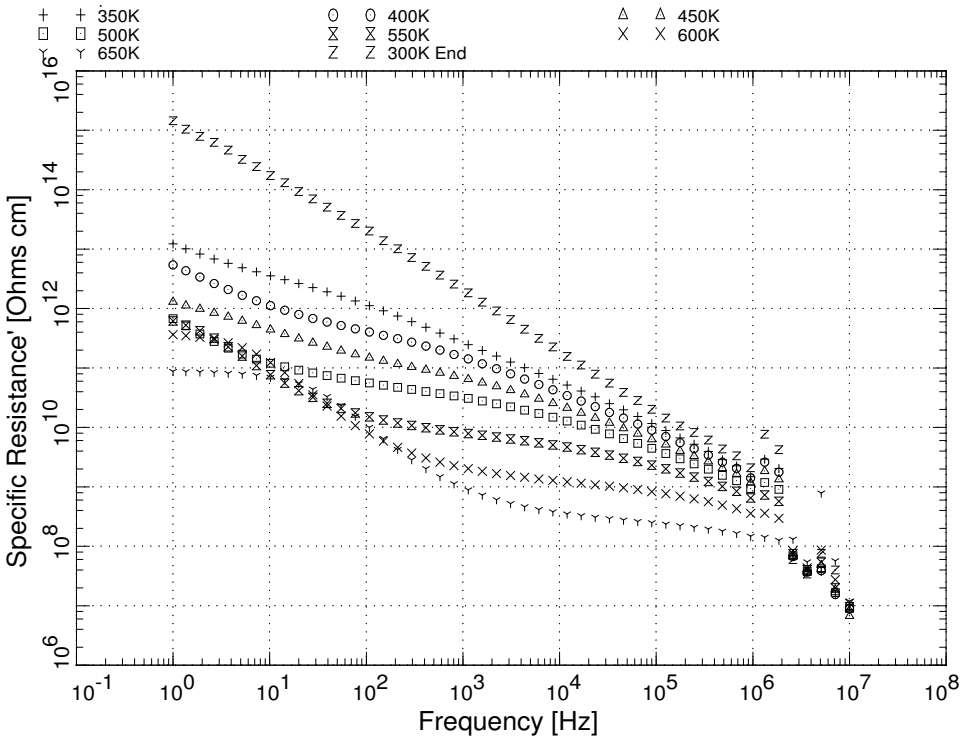

Figure 41. Resistivity of AETB tile coating of sample 1 as a function of frequency and temperature.

Figure 42. Photos showing both sides of the outer coating taken from an AETB tile. The outer surface is on the left. The inner surface (right) still show some of the white coloration of the insulating glass fibers. This sample when whole is 40 mm in diameter and 0.36 mm thick. 20 mm electrodes shown in the photos where used to test the sample fragment shown.

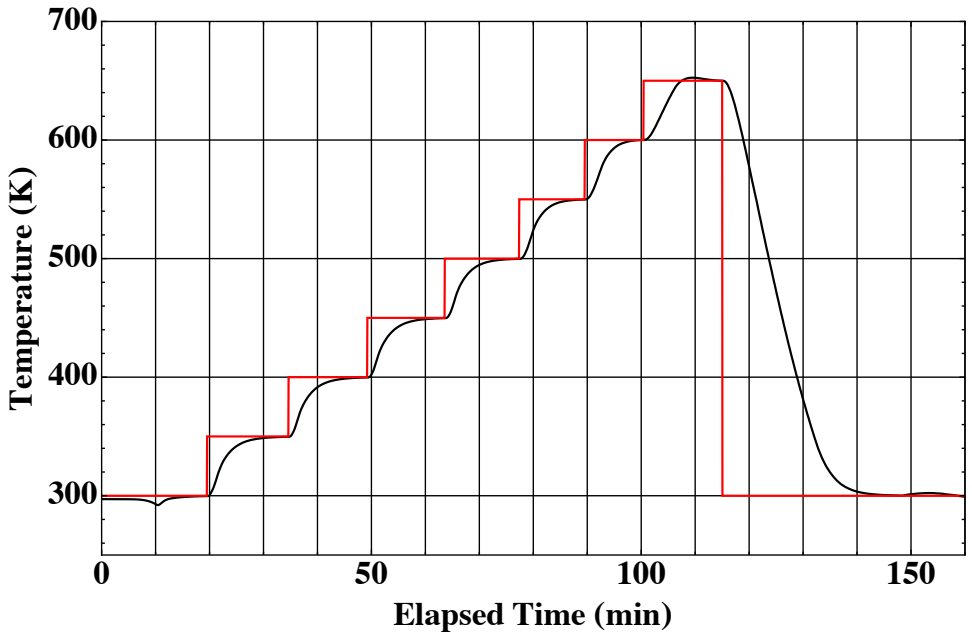

Figure 43. Temperature versus time profile for testing sample 2. The red curve shows the set temperatures, while the black shows the actual sample temperature.

imaginary portion of the permittivity measurement. The rise in permittivity below 1 kHz, in the 500K-650K curves appears to be due to a sub-1 Hertz relaxation in the tile coating that begins to show up at higher frequencies as the temperature is raised. There are corresponding slope changes in the specific resistance (although not as pronounced) at similar frequencies due to this phenomenon.

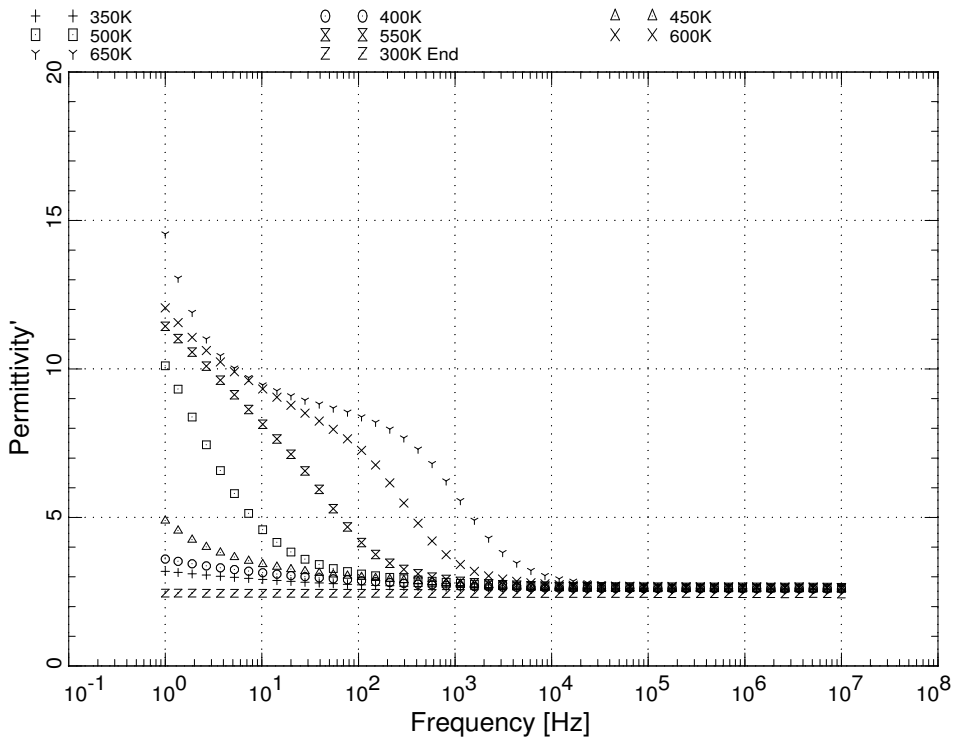

Figure 44. Permittivity of AETB tile coating of sample 2 as a function of frequency and temperature.

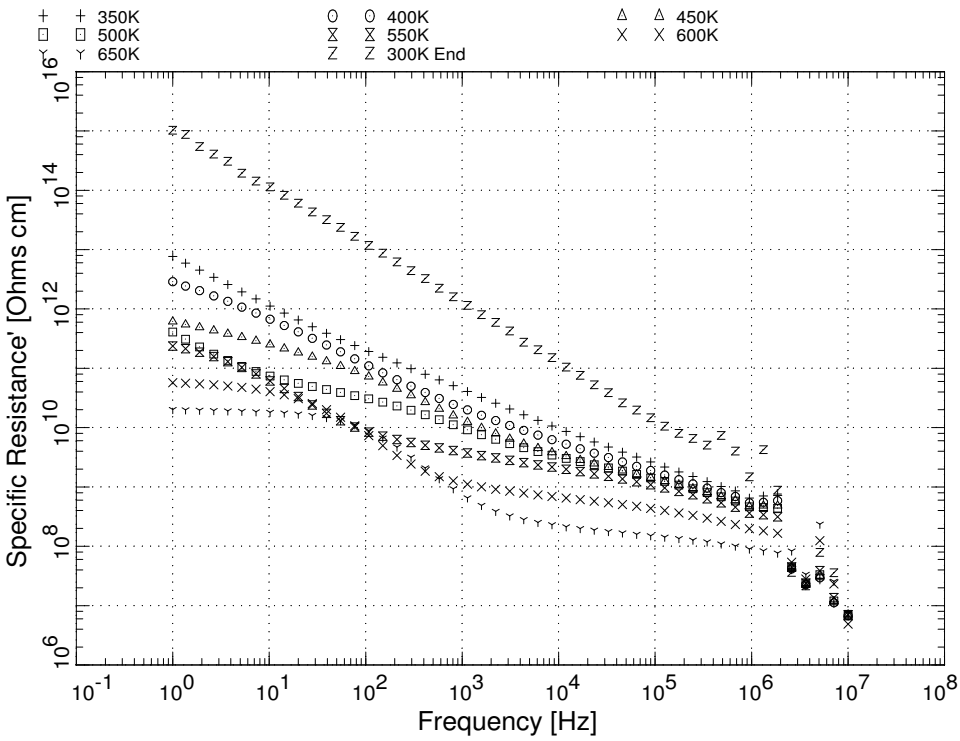

Figure 45. Resistivity of AETB tile coating of sample 2 as a function of frequency and temperature.

7 Temperature and Frequency Dependent Electrical Properties of Toughened Unipiece Fibrous Insulation (TUFI) Coating from Shuttle High-Temperature Reusable Insulation (HRSI)

The outer coating on a TUFI tile forms a gradient from the surface down into the tile. In order to see the effect this gradient has on the electrical properties, it was decided to cut samples from different depths into the tile to better characterize the electrical properties of the coating. The first three samples were taken from the regions 1-3 shown in Figure 46 below. Each of these samples is approximately 40 mm in diameter and 1.04-1.1 mm thick. A fourth sample was taken from the surface and machined as thin as possible as shown in Figure 47. This sample is around 0.82 mm thick and 40 mm in diameter. Each sample was then placed between a pair of 40 mm diameter auxiliary electrodes and measured with a Novocontrol Concept 40 Broadband Dielectric Spectroscopy system at Kennedy Space Center.

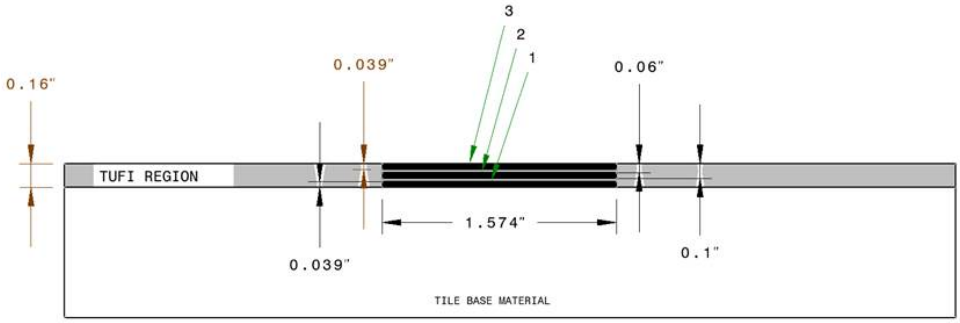

Figure 46. Diagram showing the regions 1-3 of TUFI tile coating used to create the samples for testing.

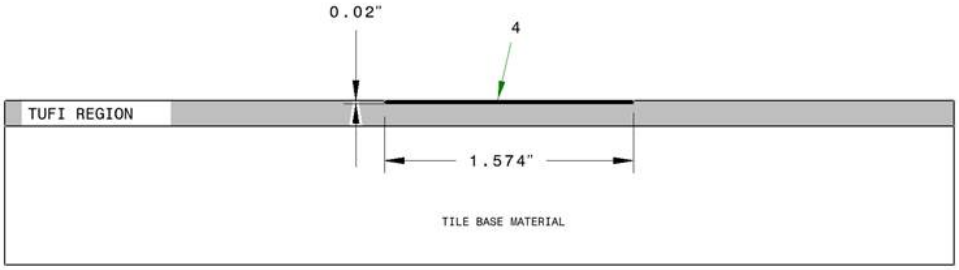

Figure 47. Diagram showing the region 4 of TUFI tile coating used to create the samples for testing the outer layer.

The dielectric spectroscopy system measures the complex capacitance of the sample using a known capacitor geometry and then derives the material proper-

ties. Typically, an insulator is represented as a complex permittivity with the real portion representing the polarizability of the material and the imaginary portion is associated with the loss mechanism (i.e, conductivity/ resistivity). This sample was measured over a frequency range from 1 Hz-10 MHz and a temperature range of 300K to 650K in steps of 50K. However, the data was very noisy in the resistivity plots above 2 MHz, so the plots have all been truncated at 2 MHz.

7.1 Region 1

The sample from region 1 is 1.03 mm thick and shows a transition from a homogeneous distribution of the coating on the top side of the sample to an inhomogeneous distribution consisting of dark areas where the outer coating clumped as it penetrated the tile. This transition can be seen in the photos of each side shown in Figure 48 below.

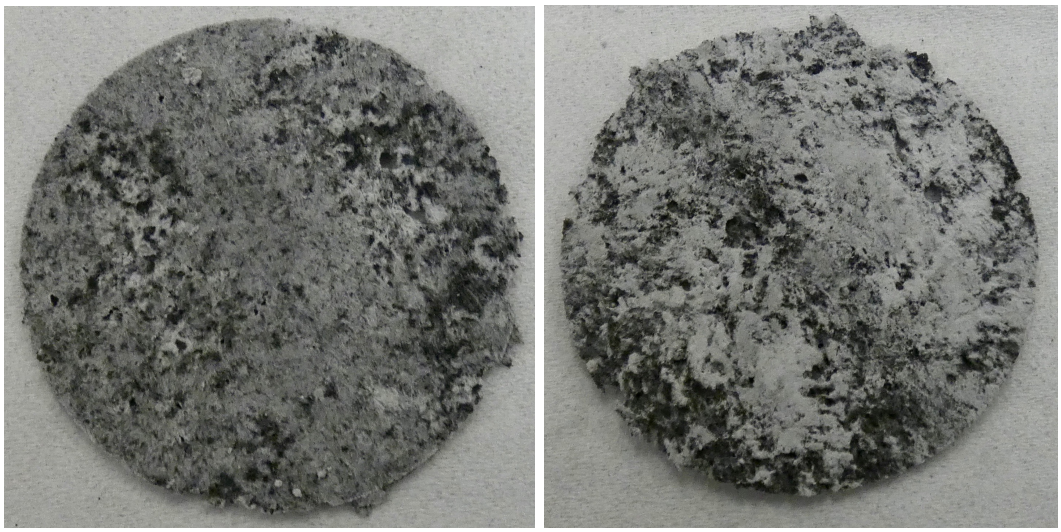

Figure 48. The left photo shows the top side of the sample and the right photo shows the underside of the sample from region 1. Notice that the top side has a more homogeneous distribution of the coating giving it a gray appearance while the underside shown on the right has light and dark regions due to some clumping of the coating material during the fabrication process.

The data shown below in Figure 49 is the real portion of the permittivity with the permittivity of free space removed (also known as the relative permittivity or the dielectric constant). Figure 50 is the specific resistance of this sample which is computed from the imaginary portion of the permittivity measurement. Both plots show the data for the sample starting at room temperature followed by the data at elevated temperatures and then ending at room temperature. This is done to see if changes occur in the material as sample bakes out. In this case, the measurements for the starting temperature of 300K and the ending temperature of 300K appear to

be similar for the permittivity but differ below 1 kHz in resistivity. This indicates that something has changed in the material due to the elevated temperature. The rise in permittivity below 100 Hz, in the 500K-650K curves appears to be due to a sub-1 Hertz relaxation in the tile coating that begins to show up at higher frequencies as the temperature is raised. There are corresponding slope changes in the specific resistance (although not as pronounced) at similar frequencies due to this phenomenon.

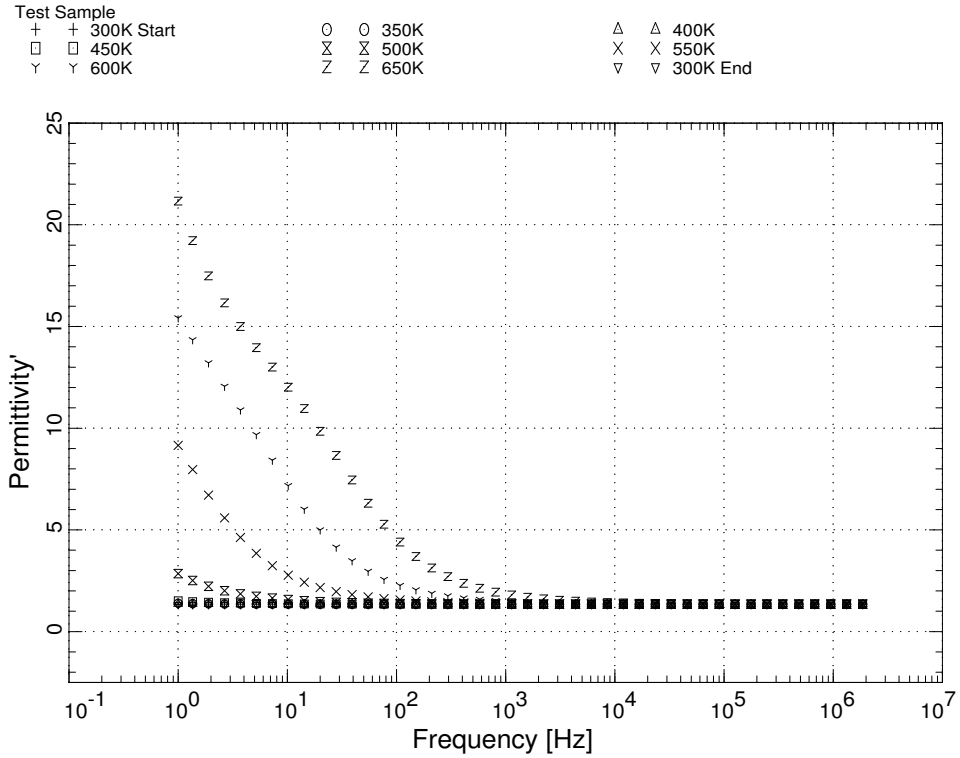

Figure 49. Permittivity of a sample from region 1 of the TUFI tile coating as a function of frequency and temperature.

7.2 Region 2

The sample from region 2 is 1.04 mm thick and has a silver/ gray appearance indicating a fairly homogeneous distribution of the coating throughout the sample (see Figure 51). However, a small amount of clumping can be seen in the photo of the sample underside.

Figure 52 shows the real permittivity and Figure 53 shows the resistivity. Once again, the rise in permittivity below 100 Hz, in the 500K-650K curves appears to be due to a sub-1 Hertz relaxation in the tile coating that begins to show up at higher frequencies as the temperature is raised. There are corresponding slope changes in the specific resistance (although not as pronounced) at similar frequencies due to

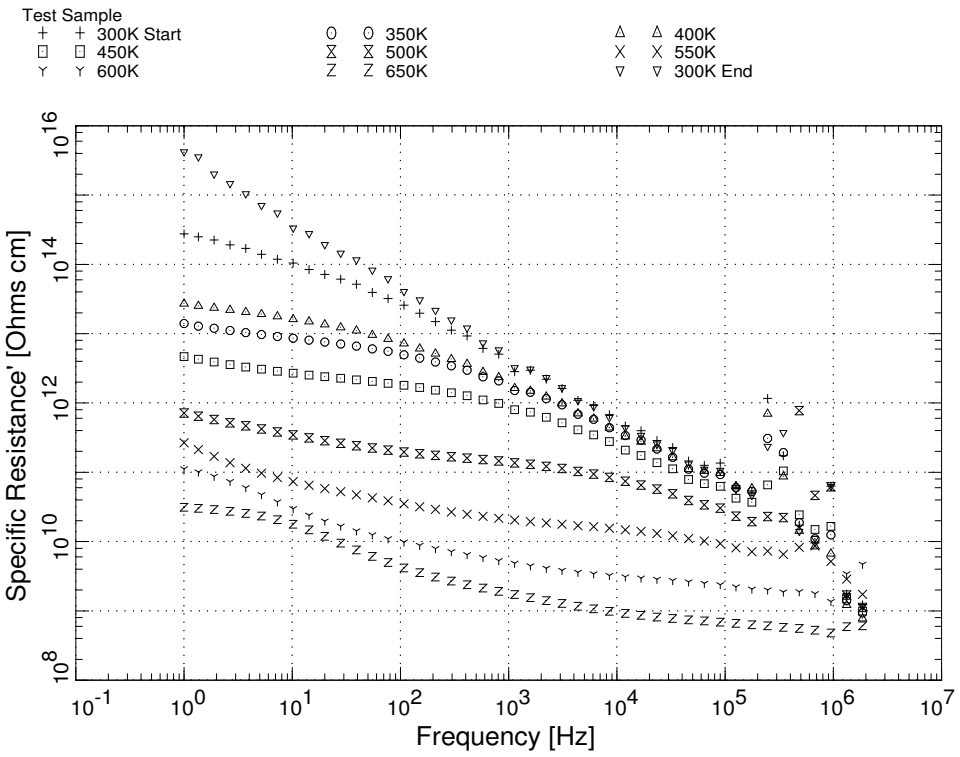

Figure 50. Resistivity of a sample from region 1 of the TUFI tile coating as a function of frequency and temperature.

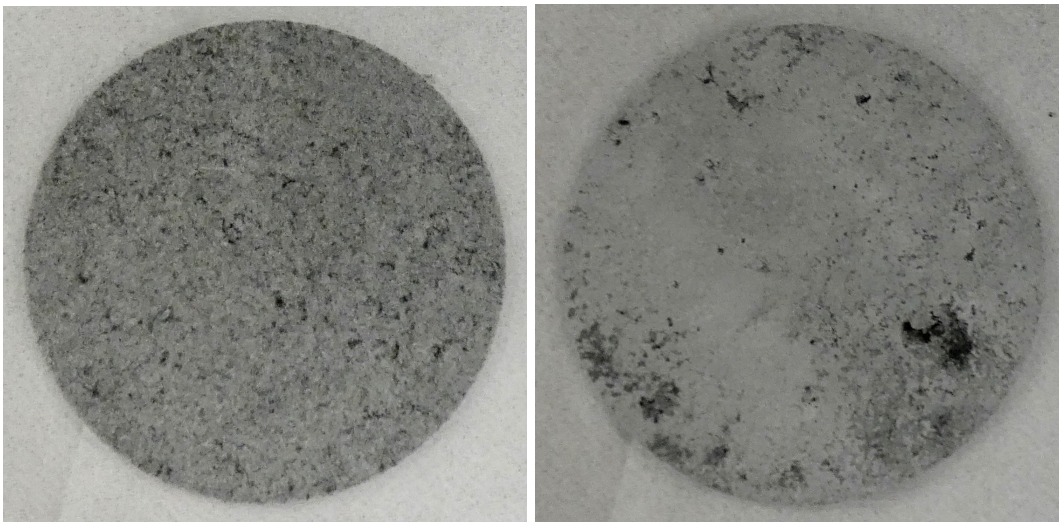

Figure 51. The left photo shows the top side of the sample and the right photo shows the underside of the sample from region 2. Both sides have a silver/ gray appearance over most of the surface indicating a fairly homogeneous distribution of the coating material. A few small areas on the underside begin to show evidence of the clumping seen the adjacent sample from region 1.

this phenomenon. The larger change in permittivity values at low frequency may be due to an increase in the density of the material in this region. Additionally, the machining process resulted in a rougher surface in region 1 than for region 2. This roughness makes it more difficult to get good electrical contact with the sample resulting in more air pockets between the electrodes and the sample. Similar changes occurred in the resistivity below 1 kHz for the starting and ending measurements at 300K.

7.3 Region 3

The sample from region 3 is 1.15 mm thick and represents the outermost portion of the coating. It has a shiny black outside and a charcoal black underside (shown in photos in Figure 54).

Figure 55 shows the real permittivity and Figure 56 shows the resistivity. Once again, the rise in permittivity below 100 Hz, in the 450K-650K curves appears to be due to a sub-1 Hertz relaxation in the tile coating that begins to show up at higher frequencies as the temperature is raised. There are corresponding slope changes in the specific resistance (although not as pronounced) at similar frequencies due to this phenomenon. The permittivity values at low frequency have dropped in comparison to the adjacent sample from region 2. Given that the sample from region 3 is less porous in appearance due to the glass like outside, one would expect the increased density to result in larger permittivity values than for region 2. It's possible that poorer electrical contact with the auxiliary electrodes may account for some of the

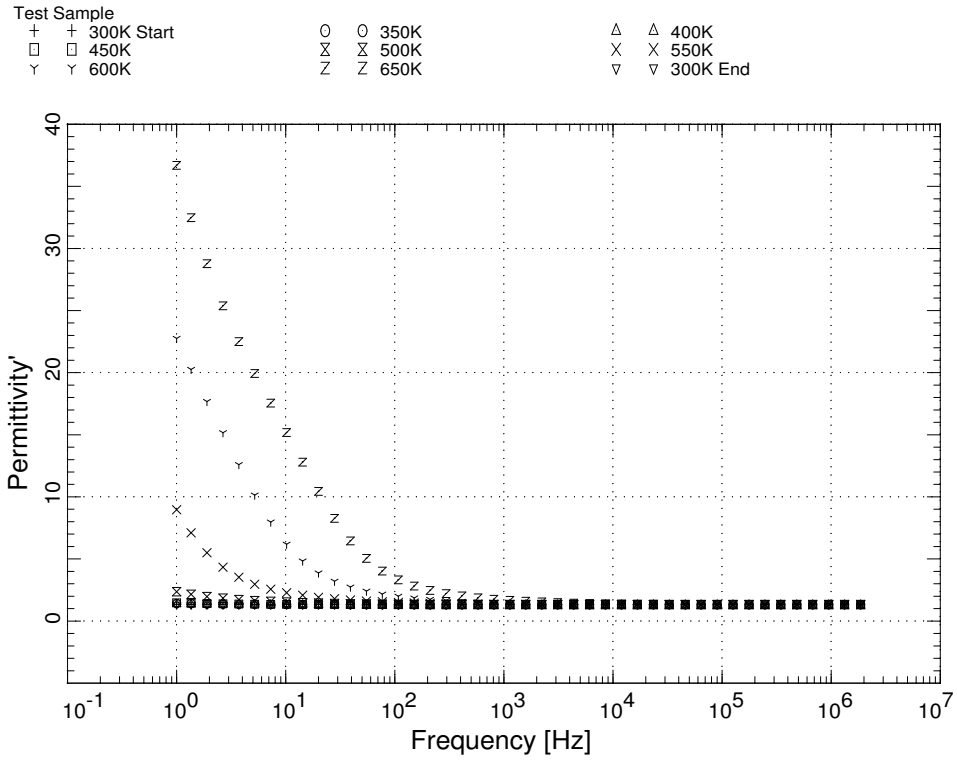

Figure 52. Permittivity of a sample from region 2 of the TUFI tile coating as a function of frequency and temperature.

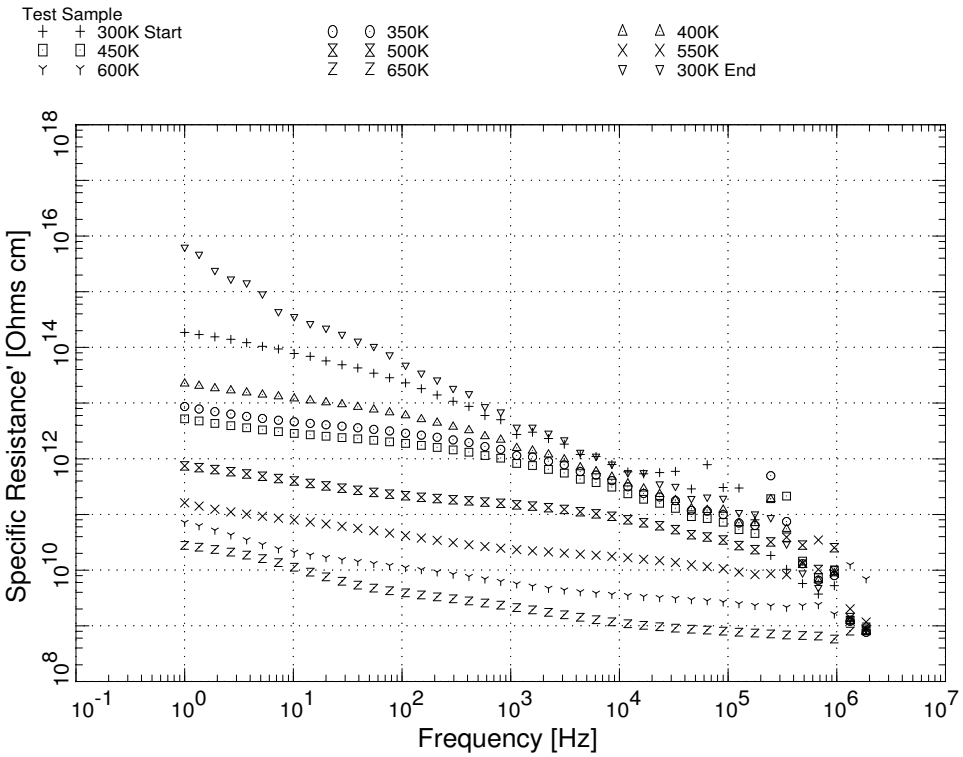

Figure 53. Resistivity of a sample from region 2 of the TUFI tile coating as a function of frequency and temperature.

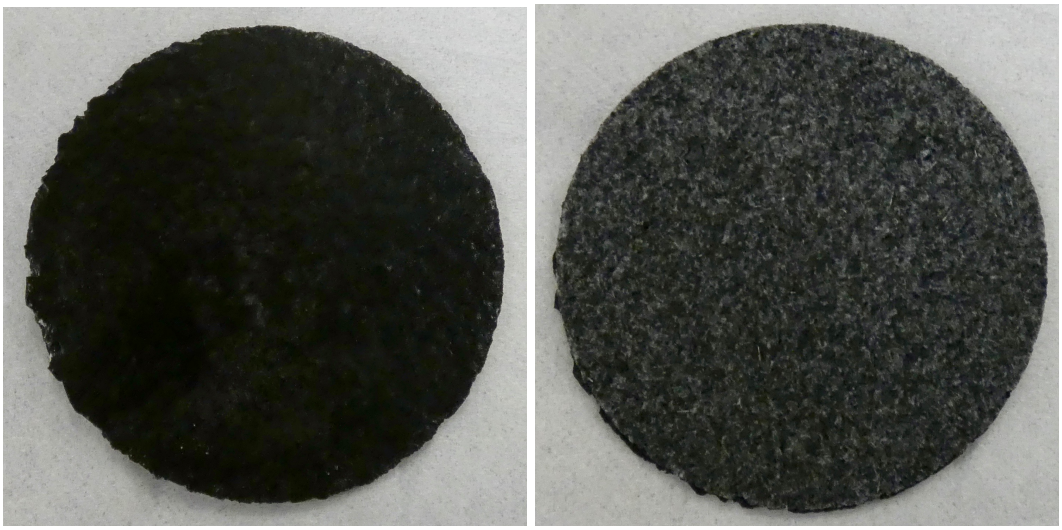

Figure 54. The left photo shows the top side of the sample from region 3 and the right photo shows the underside of the sample. These represent the outermost region of the TUFI coating.

difference. It's also possible that the outside has a slightly different chemical makeup as the fabrication process results in the smooth glass like outer layer not present in the inner samples from regions 1 and 2. The starting and ending measurements at 300K have some differences at several frequencies in the resistivity plot, but the cause is unclear.

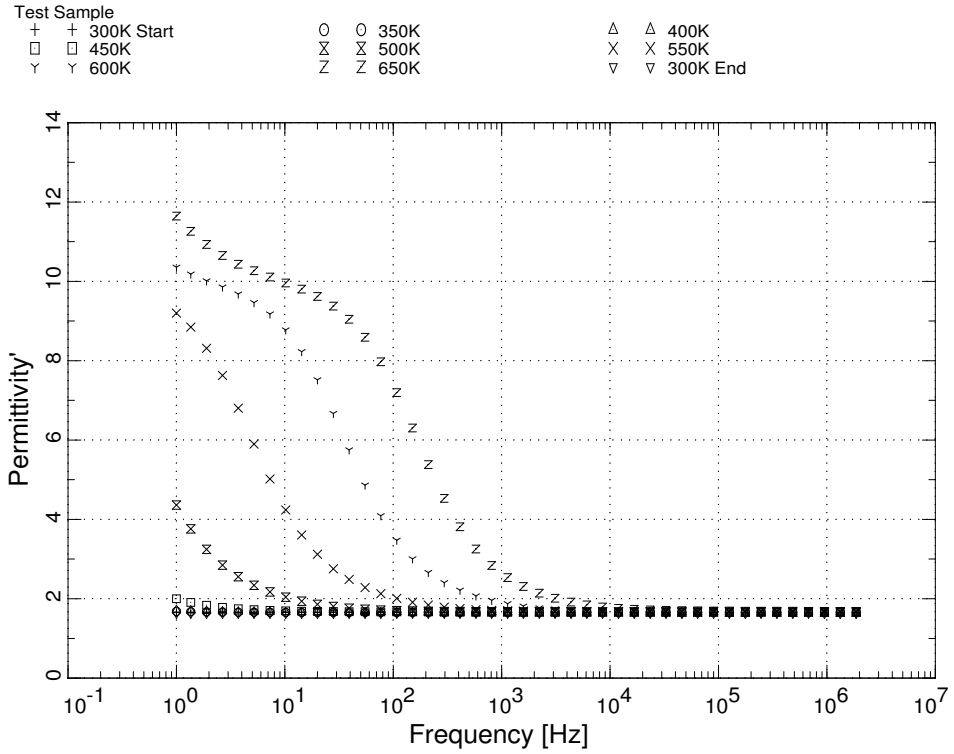

Figure 55. Permittivity of a sample from region 3 of the TUFI tile coating as a function of frequency and temperature.

7.4 Region 4

The sample from region 4 is 0.82 mm thick and represents the outermost portion of the coating. It is from a similar part of the tile as region 4, but it is thinner and will have a larger percentage of the glass like outer coating. It has a shiny black outside and a charcoal black underside (shown in photos in Figure 57).

Figure 58 shows the real permittivity and Figure 59 shows the resistivity. Once again, the rise in permittivity below 100 Hz, in the 450K-650K curves appears to be due to a sub-1 Hertz relaxation in the tile coating that begins to show up at higher frequencies as the temperature is raised. There are corresponding slope changes in the specific resistance (although not as pronounced) at similar frequencies due to this phenomenon. The permittivity values at low frequency have dropped in comparison to the similar but thicker sample from region 3. It's possible that

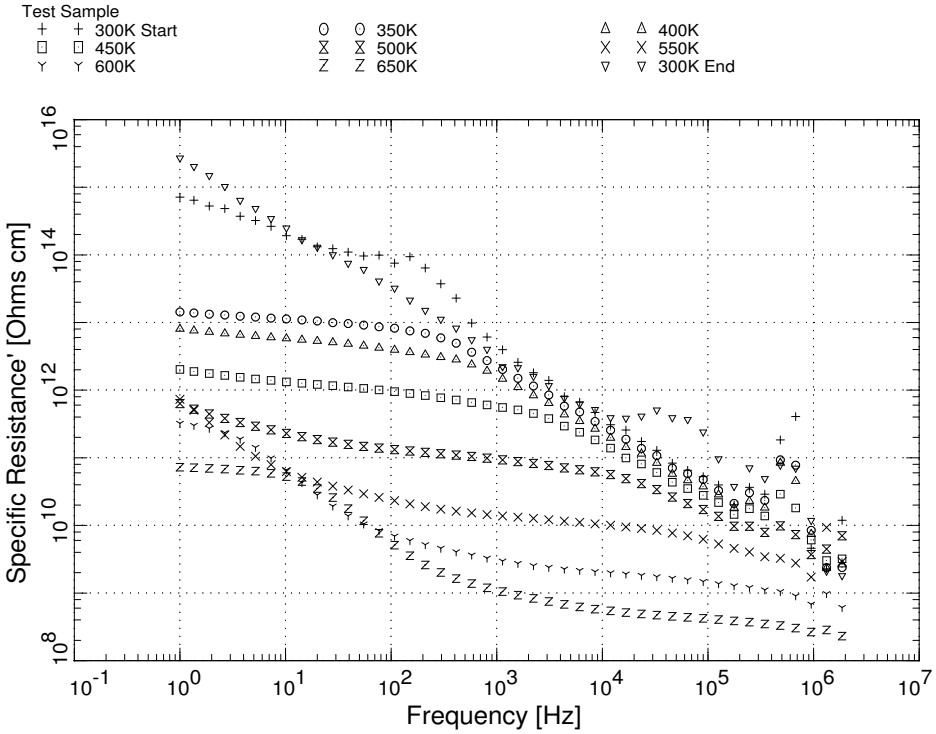

Figure 56. Resistivity of a sample from region 3 of the TUFI tile coating as a function of frequency and temperature.

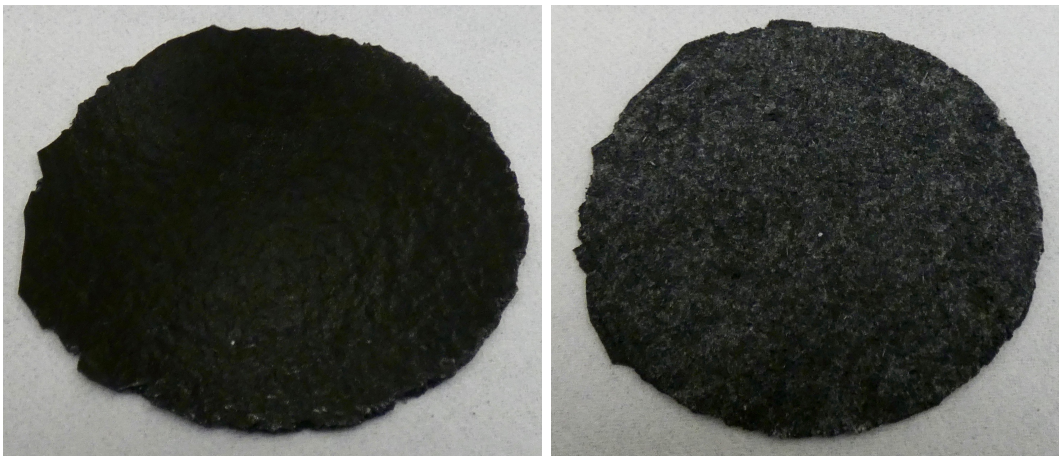

Figure 57. The left photo shows the top side of the sample from region 4 and the right photo shows the underside of the sample. These represent the outermost region of the TUFI coating, similar to region 3.

poorer electrical contact with the auxiliary electrodes may account for some of the difference. It's also possible that the shiny black outside has a slightly different chemical makeup and lower permittivity than the inside. Since the sample from region 4 has a larger fraction of this outer material, it will have a lower overall permittivity when compared to the thicker sample from region 3. The starting and ending resistivity measurements at 300K have some differences at below 10 Hz but overlap everywhere else.

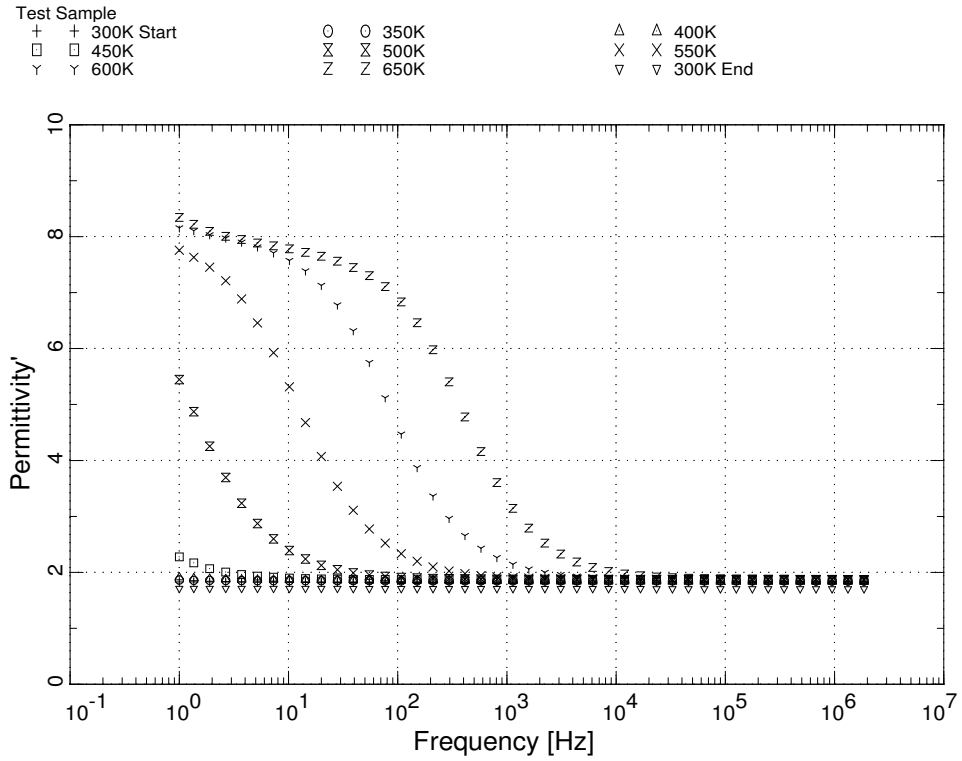

Figure 58. Permittivity of a sample from region 4 of the TUFI tile coating as a function of frequency and temperature.

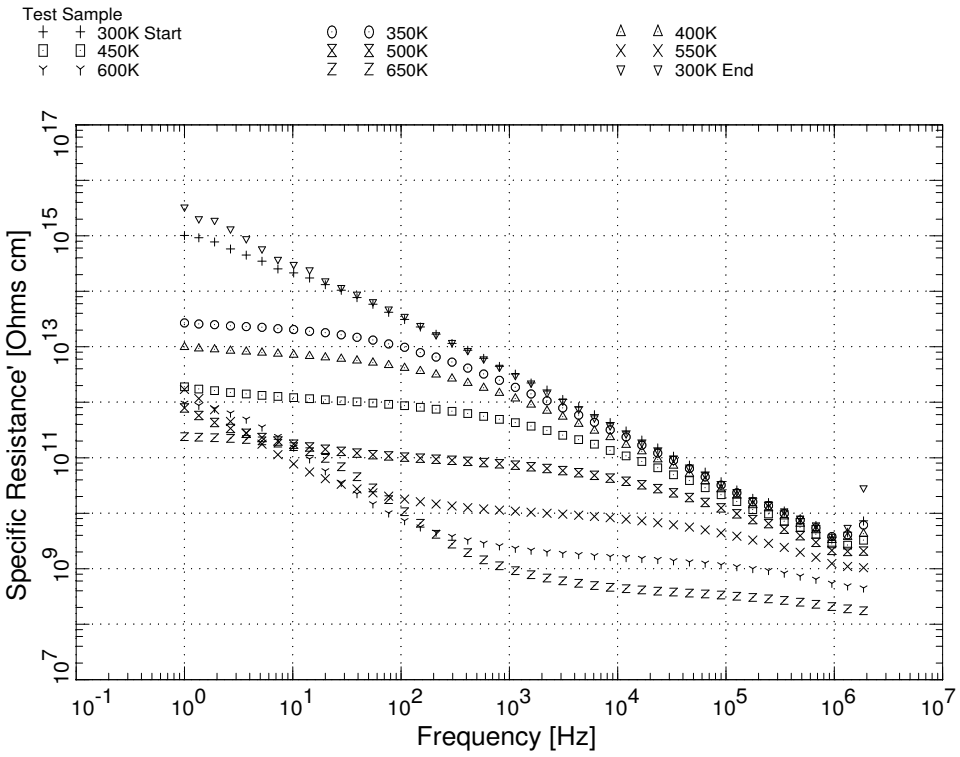

Figure 59. Resistivity of a sample from region 4 of the TUFI tile coating as a function of frequency and temperature.